PENSOFT

SENCKENBERG
world of biodiversity

Leibniz Association

Three new species of mouse spider (Araneae: Actinopodidae: *Missulena* Walckenaer, 1805) from Western Australia, including an assessment of intraspecific variability in a widespread species from the arid biome

Marleen R. Greenberg[1,2], Joel A. Huey[3], Volker W. Framenau[4,3,1], Danilo Harms[1]

1 *Zoological Museum Hamburg, Leibniz Institute for the Analysis of Biodiversity Change (LIB), Martin-Luther-King-Platz 3, 20146 Hamburg, Germany*

2 *Fachbereich Biologie, Universität Hamburg, Ohnhorststraße 18, 22609 Hamburg, Germany*

3 *Department of Terrestrial Zoology, Western Australian Museum, Welshpool, WA 6106, Australia*

4 *Harry Butler Institute, Murdoch University, 90 South Street, Murdoch 6150, Australia*

http://zoobank.org/951E28C6-EAC0-494E-BC25-5DEF1991583B

Corresponding author: Marleen R. Greenberg (marleen.greenberg@outlook.de)

Received 21 December 2020
Accepted 22 June 2021
Published 8 October 2021

Academic Editor Lorenzo Prendini

Citation: Greenberg MR, Huey JA, Framenau VW, Harms D (2021) Three new species of mouse spider (Araneae: Actinopodidae: *Missulena* Walckenaer, 1805) from Western Australia, including an assessment of intraspecific variability in a widespread species from the arid biome. Arthropod Systematics & Phylogeny 79: 509–533. https://doi.org/10.3897/asp.79.e62332

Abstract

Mouse spiders (genus *Missulena* Walckenaer, 1805) are a lineage of trapdoor spiders with males of many species having a brightly coloured red cephalic region, an abdomen that is tinged metallic blue, and the habit of wandering during the day in search of a mate. A total of 17 species of *Missulena* have been described in Australia to date but most descriptions are based exclusively on males and always small numbers of specimens. Here, we describe three new species of *Missulena* from the Pilbara and Goldfields regions of Western Australia based on morphology and genetic data: *Missulena davidi* **sp. nov.** (male and female), *M. iugum* **sp. nov.** (male) and *M. manningensis* **sp. nov.** (male). One of them is presently known only from its type locality and another one from a small range based on two specimens but *M. davidi* sp. nov. has a linear range of almost 300 km and is genetically highly structured. We use genetic data for 75 specimens as a foundation to evaluate morphological variability in this species and note substantial variation in several characters commonly used to identify species such as body size, colouration, rastellum shape and eye distances. This variation does not necessarily relate to phylogeographic structure as inferred from the genetic data, but rather seems to reflect natural variability both within and between localised populations. Overall, our results stress the need to evaluate a large series of specimens for mygalomorph taxonomy and provide an interesting example of intraspecific variability in hard-to-collect species that are usually underrepresented in museum collections.

Key words

Mygalomorphae, Pilbara, speciation, phylogeny, systematics, taxonomy

1. Introduction

Mouse spiders (genus *Missulena* Walckenaer, 1805) are a lineage of trapdoor spiders from Australia and Chile. They are ambush hunters and build burrows that are lined with silk and usually sealed with one or more lids (Main 1956). At least some species are known to balloon, which is a rather rare behaviour amongst mygalomorph spiders (Buzatto et al. 2021; Main 1956, 1976). Unlike other trapdoor spiders (Mygalomorphae), at least within an Australian context, the males of many mouse spider species have been recorded to wander during the day in search of a mate. Possibly correlated with this diurnal activity pattern, they have striking colour patterns, such as a red or orange cephalic region and metallic or iridescent patterning on the abdomen (Framenau et al. 2014; Harms and Framenau 2013; Miglio et al. 2014). Females and juveniles are not as colourful (Fig. 1C, D) and their cryptic burrows usually have one or two floppy lids without trap lines, are covered by loose silk on the inside, and usually concealed in leaf litter (Fig. 1A, B, E). The bright colouration of some (but not all) male *Missulena* sets them apart from their close relatives, the Australian funnel-web spiders (family Atracidae) (Hedin et al. 2018), although both groups share potent venoms that are known to be medically-significant in humans and other primates (Gunning et al. 2003; Nicholson et al. 1998; Palagi et al. 2013). Severe bites have only been recorded for the males of a few species and bites are generally 'dry' (Isbister 2004; Rash et al. 2000). Currently, there are 17 described species of *Missulena* from Australia in addition to one species from Chile (Framenau and Harms 2017; World Spider Catalog 2020) although many more species are known from Australian collections, particularly from the arid biome of Western Australia (e.g., Castalanelli et al. 2014; Framenau and Harms 2017).

Species delineation in mygalomorph spiders can be challenging because many species are difficult to collect, morphologically conservative, and the taxonomic framework for species identification is often poor (e.g., Bond and Stockman 2008; Cooper et al. 2011; Starrett and Hedin 2007; Wong et al. 2017). In the case of *Missulena*, most species descriptions are several decades old (e.g., Wormersley 1943) and have relied on single or very few male specimens. Females have never been adequately illustrated and diagnosed. Therefore, almost all diagnostic characters used to distinguish species, such as the shape of the pedipalp and embolus, or tibial length/width ratios, are taken from males (e.g., Faulder 1995). Species distributions have been very difficult to delineate although the recent descriptions (Harms and Framenau 2013; Miglio et al. 2014; Framenau and Harms 2017) and comprehensive genetic datasets that were generated as part of larger DNA barcoding projects (Castalanelli et al. 2014) have suggested that most (but not all) species have small distribution ranges.

In this paper, we describe three new species of *Missulena* from central and north-western Western Australia. Two of these new species follow the "typical" pattern of rarity in research collections and taxonomic descriptions that are based on a few males from single localities, although the morphological descriptions are backed up by a molecular phylogenetic framework. A third species is interesting insofar as it seems to be widespread across a wide area in north-western Australia, is morphologically and genetically variable across its range, and commonly collected. We use *Missulena davidi* sp. nov. not only to document female morphology based on a large sample size for the first time in this genus, but also to assess morphological variability of taxonomic key features in light of a sound molecular phylogenetic framework. A qualitative description of the morphological characters that are rather conserved versus those that show substantial variability within species will aid future species descriptions.

2. Materials and methods

2.1. Molecular work

There were 89 *Missulena* cytochrome *c* oxidase I (COI) sequences available on GenBank, produced by previous studies (Castalanelli et al. 2014; Harms and Framenau 2013; Framenau and Harms 2017). These sequences were supplemented by 78 additional *Missulena* specimens from the Western Australian Museum, producing an ingroup dataset of 167 specimens. These specimens had DNA extracted, amplified, and sequenced following the protocols outlined in Harvey et al. (2018). Sequences and analyses were managed in Geneious Prime (Biomatters Ltd). All new sequences were uploaded to GenBank and are listed in Supplementary Material 1.

The 167 *Missulena* sequences were aligned with two outgroup taxa, a specimen of *Actinopus* KY017543 (family Actinopodidae) and a specimen of *Atrax* KY017748 (Atracidae). Recent phylogenetic studies have shown that Atracidae is closely related to Actinopodidae (Hedin et al. 2018). The final 169 sequence COI dataset was aligned using the MAFFT plugin in Geneious Prime (Katoh and Standley 2013). A Maximum Likelihood phylogeny was built using the RaXML plugin in Geneious Prime (Stamatakis 2006), using the GTR+G substitution model, with 1000 bootstrap replicates.

2.2. Morphology

All specimens chosen for morphological study belong to a monophyletic group comprising 70 specimens that was recovered by the phylogenetic analyses (Fig. 2). Within this group, one large monophyletic clade from the central Pilbara region (here recognised as a new species, *Missulina davidi* sp. nov.) was genetically highly structured. Three specimens from Mt. Ida (2 specimens) and Mt. Manning (1 specimen) performed as the sister-group to this clade and are recognized here as two different species, *M. iugum* sp. nov and *M. manningensis* sp. nov., respectively.

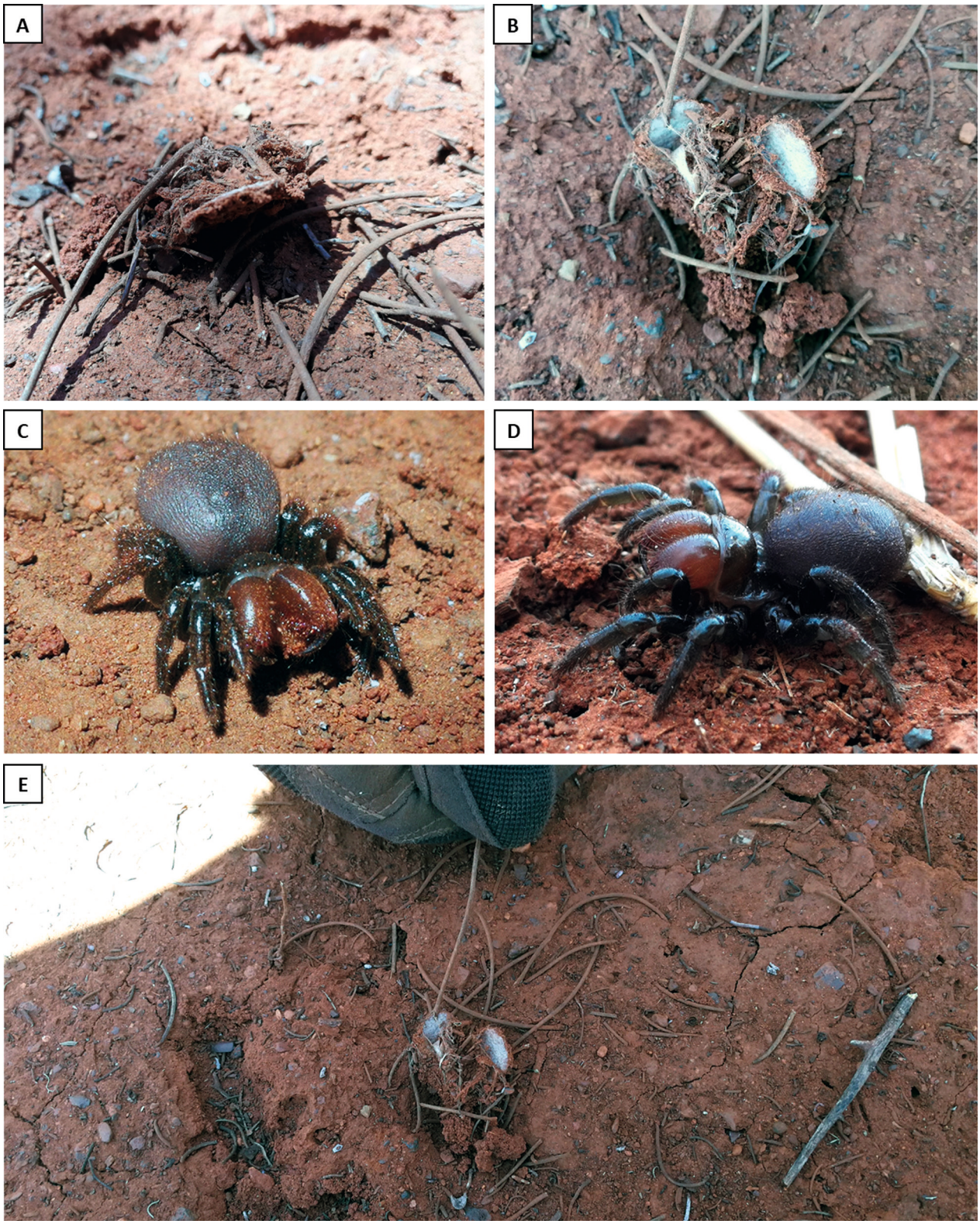

Figure 1. *Missulena davidi* sp. nov., photos of **A B E** burrow structure with two openings; **C D** female. Photos taken near Newman, Western Australia (Copyright: D. Harms, 2019).

We selected 26 adult females and 12 adult males of sequenced *M. davidi* sp. nov. from across the species range and assessed a total of 34 morphological characters, four of these qualitative (e.g., body colouration) and 30 quantitative (e.g., body measurements and spine count of the rastellum). All specimens are deposited at the Western Australian Museum in Perth, Australia (WAM), and the Harry Butler Institute, Murdoch University, Perth, Australia (HBI).

A Leica DM4500 digital camera attached to a Leica M205A stereomicroscope and controlled by the Leica Application Suite X Version 3.0.1. was used for examination and morphological measurements in millimetres. Digital images were taken with a BK Plus Lab System by

Figure 2. Maximum Likelihood phylogeny of all *Missulena* specimens. The ultimate outgroup taxon *Atrax* has been removed from the figure for convenience. All bootstrap values below 80 have been removed. Genetic clades within *Missulena davidi* sp. nov. are colour-coded: clade I brown, clade II red, clade III blue, clade IV pink.

Dun, Inc. with integrated Canon EOS 5D Mark III and the program Capture One 9, or with a Hitachi TM4000Plus scanning electron micrograph (SEM). The images were stacked with Zerene stacking software (Zerene Systems LLC 2018). The drawings were created with the help of printed images that were traced on a Comicstar light table and scanned afterwards. Images were edited with Adobe Photoshop CS6. Maps were created using QGIS Version 3.0.

Box-Whisker-Plots for carapace and eye variation measurements as well as rastellum counts in *M. davidi* sp. nov. were compiled in RStudio Version 1.2.1335 (RStudio, Inc). For the comparison of leg spination and cheliceral dentition five specimens of each sex were examined in detail. The cuspules on the maxillae and labium were counted in the ventral position and represent minimum values because not all cuspules near the joints could be seen clearly. Carapace height was measured laterally from the highest point of the carapace vertically to the edge of the carapace.

Abbreviations used in the taxonomic sections are as follows: **OQ** ocular quadrangle, **AME** anterior median eyes, **ALE** anterior lateral eyes, **PME** posterior median eyes, **PLE** posterior lateral eyes, **PLS** posterior lateral spinnerets, **PMS** posterior median spinnerets, **rl** retrolateral, **v** ventral, **pl** prolateral, **d** dorsal.

3. Taxonomy

Family Actinopodidae Simon, 1892

Genus *Missulena* Walckenaer, 1805

Missulena Walckenaer, 1805: 8. Type species: *Missulena occatoria* Walckenaer, 1805, by monotypy.

Eriodon Latreille, 1806: 85. Type species: *Eriodon occatorius* Latreille, 1806, by monotypy. Synonymised by Simon 1903: 877.

3.1. *Missulena davidi* sp. nov.

http://zoobank.org/8B7D21DD-872B-4C09-8776-7B7FAD1C-BE57

Figs 3–7

Type material. Holotype: AUSTRALIA – Western Australia • ♂; Juna Downs Station, 113 km NW of Newman; 22°41.23′S 118°53.55′E; 10 May 2011; C. Cole and P. Runham leg.; pit trap; WAM T119725 • **Allotype**: AUSTRALIA – Western Australia • ♀; Hope Downs, 73.7 km NW of Newman; 20°59.42′S 119°7.3′E; 27 June 2010; G. Humphreys and P. Runham leg.; dug from burrow; WAM T107393 • **Paratypes**: AUSTRALIA – Western Australia • 1♀; same data as holotype; 22°41.18′S 118°53.58′E; dug from burrow; WAM T119711 • 1♀; Juna Downs Station, 114 km NW of Newman; 22°43.55′S 118°50.98′E; 12 May 2011; P. Runham leg.; dug from burrow; WAM T119718 • 1♂; Juna Downs Station, 116 km NW of Newman; 22°38.73′S 118°54.17′E; 11 May 2011; C. Cole and P. Runham leg.; pit trap; WAM T119726 • 1♂; same data as for preceding; WAM T119727 • 1♂; same data as for preceding; 10 May 2011; WAM T119728 • 1♂; same data as for preceding; WAM T119729 • 1♂; same data as for preceding; 117 km NW of Newman; 22°37.73′S 118°54.1′E; WAM T119731 • 1♂; same data as for preceding; 22°36.63′S 118°56.38′E; G. Humphreys and J. Tatler leg.; WAM T119733.

Other material examined. AUSTRALIA – Western Australia • 1♀; Carnarvon, 99 Gascoyne Road; 24°53′S 113°39′E; 23 July 2002; residents leg.; by hand; WAM T46798 • 1♂; Cloudbreak Mining Lease, Fortescue Metals Group (site 25); 22°20.1′S 119°24.23′E; 6 Sept. 2006; S. Thompson leg.; WAM T84005 • 1♀; Jimblebar minesite, 35 km E of Newman; 23°22.5′S 120°12.58′E; 6 Feb. 2009; P. Bolton and C. Weston leg.; active search; WAM T95397 • 1♀; Murray Hills, Mulga Downs Station, Ecologia project 1142; 22°07.67′S 118°30.92′E; 19 Apr. 2009; N. Dight and L. Quinn leg.; dry pitfall trap; WAM T97637 • 1♀; Davidson Creek, ca. 75 km E of Newman, vert site 6; 23°25.73′S 120°26.8′E; 9 Apr. 2010; J. Clark leg.; dry pitfall; WAM T102165 • 1♀; South Parmelia, 52 km NW of Newman; 23°5.13′S 119°19.08′E; 16 Apr. 2011; R. Teale and M. Greenham leg.; dug from burrow; WAM T113591 • 1♂; Southern Flank, 72 km NW of Newman; 23°0.17′S 119°8.37′E; 14 Apr. 2011; R. Teale and M. Greenham leg.; dug from burrow; WAM T113596 • 1♂; same locality; 23°0.18′S 119°8.35′E, 14 Apr. 2011; R. Teale and M. Greenham leg.; dug from burrow; WAM T113598 • 1♀; 113.8 km NW of Newman; 22°39.39′S 118°55.09′E; 26 May 2011; M. Greenham and R. Teale leg.; dug from burrow; WAM T113626 • 1♀; 119.1 km NW of Newman; 22°38.02′S 118°52.19′E; 30 May 2011; M. Greenham and R. Teale leg.; dug from burrow; WAM T113660 • 1♀; 117.6 km NW of Newman; 22°37.66′S 118°53.76′E; 31 May 2011; M. Greenham and R. Teale leg.; dug from burrow; WAM T113665 • 1♀; Mudlark, 107 km W of Newman; 23°5.63′S 118°43.17′E; 30 June 2011; C. Cole and N. Watson leg.; dug from burrow; WAM T116746 • 1♀; Mudlark, 111 km WNW of Newman; 23°5.2′S 118°41.18′E; 30 June 2011; M. Greenham and J. Cairnes leg.; dug from burrow; WAM T116751 • 1♀; same data as for preceding; 23°5.22′S 118°41.17′E; WAM T116755 • 1♀; Mudlark, 113 km W of Newman; 23°2.28′S 118°40.97′E; 1 July 2011; M. Greenham and J. Cairnes leg.; dug from burrow; WAM T116776 • 1♀; Mudlark, 102 km W of Newman; 23°5.4′S 118°48.67′E; 3 July 2011; C. Cole and N. Watson leg.; dug from burrow; WAM T116839 • 1♀; Mudlark, 94 km W. of Newman; 23°4.78′S 118°51.48′E; 6 July 2011; M. Greenham and J. Cairnes leg.; dug from burrow; WAM T116866 • 1♀; same locality; 23°4.77′S 118°51.47′E; 26 July 2011; C. Cole and N. Watson leg.; dug from burrow; WAM T116868 • 1♀; 84.2 km NW of Newman; 22°40.5′S 119°20.95′E; 26 July 2011; D. Kamien, M. Greenham and Z. Hamilton leg.; dug from burrow; WAM T116873 • 1♀; same data as for preceding; 22°40.48′S 119°20.9′E; WAM T116874 • 1♀; same data as for preceding; 89.3 km NW of Newman; 22°38.45′S 119°19.23′E; WAM T116875 • 1♀; same data as for preceding; 89.3 km NW. of Newman; 22°38.45′S 119°19.22′E; WAM T116881 • 1♀; Mulga Downs Station, Cowra, site 994-13; 22°13.63′S 119°0.82′E; 16 Apr. 2012; WAM T118328 • 1♀; 84.8 km NW of Newman; 22°40.1′S 119°22.48′E; 27 July 2011; D. Kamien, M. Greenham and Z. Hamilton leg.; dug from burrow; WAM T119975 • 1♀; same data as for preceding; 99.1 km NW of Newman; 22°34.3′S 119°17.15′E; WAM T119979 • 1♀; same data as for preceding; 22°34.3′S 119°17.17′E; WAM T119980 • 1♀; 105.3 km NW of Newman; 22°30.72′S 119°15.55′E; 28 July 2011; D. Kamien, M. Greenham and Z. Hamilton leg.; dug from burrow; WAM T119984 • 1♀; same data as for preceding; 22°30.72′S 119°15.53′E; WAM T119993 • 1♀; 81.2 km NW of Newman; 22°42.02′S 119°22.68′E; 29

July 2011; D. Kamien, M. Greenham and Z. Hamilton leg.; dug from burrow; WAM T119995 • 1♀; 85.2 km NW. of Newman; 22°39.2′S 119°24.82′E; 31 July 2011; D. Kamien, M. Greenham and Z. Hamilton leg.; dug from burrow; WAM T120018 • 1♀; same data as for preceding; 22°39.2′S 119°24.83′E; WAM T120019 • 1♂; same data as for preceding; 18.9 km NE of Tom Price; 22°39.2′S 119°24.82′E; WAM T120081 • 1♀; Koodaideri Corridor West, 93.7 km NE of Tom Price; 22°19.7′S 118°36.61′E; 20 Feb. 2012; C. Cole leg.; burrow search; WAM T122209 • 1♀; same data as for preceding; 89.4 km NE of Tom Price; 22°15.92′S 118°31.3′E; WAM T122217 • 1♀; same data as for preceding; 71.7 km NE of Tom Price; 22°8.12′S 118°8.17′E; WAM T122224 • 1♀; same data as for preceding; 70.1 km NE of Tom Price; 22°9.31′S 118°8.07′E; WAM T122226 • 1♀; same data as for preceding; 22°9.37′S 118°8.07′E; leaf litter rake; WAM T122235 • 1♀; same data as for preceding; 82.1 km NE of Tom Price; 22°13.95′S 118°24.88′E; burrow search; WAM T122252 • 1♀; same data as for preceding; 77.3 km NE of Tom Price; 22°1.68′S 118°0.22′E; WAM T122254 • 1♀; 111.6 km NW of Newman; 22°53.52′S 118°45.89′E; 29 Mar. 2012; C. Cole and N. Watson leg.; dug from burrow; WAM T122822 • 1♀; 115.4 km NW of Newman; 22°54.52′S 118°43.05′E; 31 Mar. 2012; C. Cole and N. Watson leg.; dug from burrow; WAM T122843 • 1♀; 118.6 km NW of Newman; 22°52.85′S 118°41.22′E; 1 Apr. 2012; N. Watson and P. Brooshooft leg.; dug from burrow; WAM T122865 • 1♀; 124 km NW of Newman; 22°51.93′S 118°38.47′E; 1 Apr. 2012; N. Watson leg.; dug from burrow; WAM T122872 • 1♂; 63.5 km ESE of Paraburdoo, site 1000-tur01; 23°17.31′S 118°17.1′E; 27 Apr. 2012; E.S. Volschenk leg.; wet pitfall; WAM T125176 • 1♀; Koodaideri Western Corridor, 217.5 km NW of Newman; 22°7.71′S 118°5.57′E; 28 Mar. 2012; G. Humphreys and M. Greenham leg.; dug from burrow; WAM T125307 • 1♀; same data as for preceding; 194.8 km NW of Newman; 22°7.71′S 118°7.71′E; WAM T125308 • 1♀; Koodaideri Western Corridor, 214 km NW of Newman; 22°8.14′S 118°6.46′E; 29 Mar. 2012; G. Humphreys and J. King leg.; dug from burrow; WAM T125316 • 1♀; 118.2 km NW of Newman; 22°36.32′S 118°55.15′E; 19 Nov. 2011; M. Greenham and Z. Hamilton leg.; WAM T126257 • 1♀; 118.3 km NW of Newman; 22°36.67′S 118°54.43′E; 18 Nov. 2011; M. Greenham and Z. Hamilton leg.; WAM T126260 • 1♀; same data as for preceding; WAM T126264 • 1♀; 114 km NW of Newman; 22°36′54″S 118°57′18″E; 21 Nov. 2011; M. Greenham and Z. Hamilton leg.; WAM T126272 • 1♀; same data as for preceding; 22°36.87′S 118°57.3′E; WAM T126276 • 1♀; Karijini National Park, ca. 20 km SW of Hancock Gorge; 22°29.03′S 118°8.85′E; 15 Mar. 2015; C. Stevenson, M.S. Harvey and M. Hillyer leg.; WAM T135548 • 1♀; Karijini National Park, ca. 25 km SSW. of Dales Gorge; 22°39.48′S 118°26.05′E; 17 Mar. 2015; M.S. Harvey et al. leg.; WAM T135563 • 1♀; Karijini National Park, ca. 6 km NW of Mt Bruce; 22°34.12′S 118°5.98′E; 15 Mar. 2015; J. Huey et al. leg.; WAM T135591.

Diagnosis. Males of *Missulena davidi* sp. nov. share the red colouration of chelicerae and pars cephalica with *M. langlandsi* Harms and Harvey, 2013, *M. occataria* Walckenaer, 1805, *M. insignis* O. Pickard-Cambridge, 1877, *M. iugum* sp. nov. and *M. manningensis* sp. nov. that are morphologically most similar. They differ from *M. langlandsi* by having strong, conical spines of the rastellum (thin and not conical in the former) and a longer carapace (>3.00 mm; *M. langlandsi* up to 2.8 mm). They differ from *M. occataria* and *M. insignis* by having spines on patellae III and IV only and not on all four legs (on patellae I and II 1 spine, respectively). *Missulena davidi* sp. nov. males have more cuspules on maxillae and labium than those of *M. manningensis* sp. nov. (*M. manningensis* sp. nov.: 5 at labium, 30 at maxillae; *M. davidi* sp. nov.: 15–10 at labium, 35–100 at maxillae). *Missulena davidi* sp. nov. males differ from *M. iugum* sp. nov. by the ridge present in the cheliceral groove. Females of *Missulena davidi* sp. nov. have uniformly red chelicerae that they share with *M. insignis*; however, the fourth leg of *M. davidi* sp. nov. is the longest of all legs, whilst in *M. insignis* the longest leg is the first. Additionally, there are no cuspules recorded on the labium or the maxillae in *M. insignis* females.

Description. MALE (based on holotype; WAM T119725). Total length 9.8. **Colour**: pars cephalica and chelicerae reddish-orange (Fig. 3C); a slim, black ring surrounding the PME (Fig. 4E); pars thoracica brown with a light, metallic blue sheen (Fig. 3C); abdomen greyish with a strong, metallic blue sheen on the dorsal side, ventrally more brownish with a faint hint of purple (Fig. 3D, E); sternum orange, slightly fading into olive with 8 sigilla in similar colour (Fig. 4D); labium and maxillae orange with a dark olive spot on the base of labium (Fig. 3F); legs olive-yellowish fading into light brown ventrally, dorsally brown (Fig. 3A, B); spinnerets beige-coloured (Fig. 3E). **Carapace**: 3.86 long and 4.67 wide; clypeus 0.31; pars cephalica covers 2.45 of its length, is highly elevated and slightly granulated with very few setae (Fig. 3G); pars thoracica also granulated with bands of faint, radial fissures and with two notches close to the abdomen (Fig. 3C). **Eyes**: OQ 4 times wider than long; outer width of each eye pair AME 0.66, ALE 2.44, PME 1.48 and PLE 2.21; diameter of AME 0.19, ALE 0.22, PME 0.15, PLE 0.19; anterior eyes very slightly recurved; posterior eyes strongly recurved (Fig. 4E). **Chelicerae**: 2.04 long and 1.47 wide on the base; edges rounded and recurved with the widest point being 1.55 close to the chelicerae base (Fig. 3C); small, faint files along the outer margin of each chelicera; evenly spread setae along the inner margin and the anterior part of the chelicerae; rastellum present, slightly pronounced, consisting of a sclerotized process with 7 (left 8) strong, conical spines (Fig. 4F); over 25 setae cover the anterior base of fang of each chelicera; inner margin of cheliceral furrow with 2 rows of teeth and a general cheliceral teeth area in between those 2 clear rows (Fig. 4A, J); prolateral row with approx. 9 teeth; retrolateral row with 4 teeth; intermediate area with 10 small teeth. **Maxillae**: 2.08 long and 1.44 wide; at least 80–100 weakly developed cuspules along entire anterior margin (Fig. 3F). **Labium**: 0.96 long and 0.86 wide on the base; conical; at least 40 weakly developed cuspules anteriorly (Fig. 3F); labiosternal junction visible (Fig. 4D). **Sternum**: 2.6 long and 2.38 wide; ovoid (Fig. 4D); setae of various length somewhat densely but disordered along the margin and a smaller amount of setae spread unevenly over the sternum; 4 pairs of sigilla, anterior pair smallest and hardly visible, second pair also very small and circular, third pair significantly larger than second (roughly 5 times bigger) in the shape of an elongated oval, and posterior pair biggest (roughly 1.5 times the size of the third pair) in the shape of a drop, all sigilla

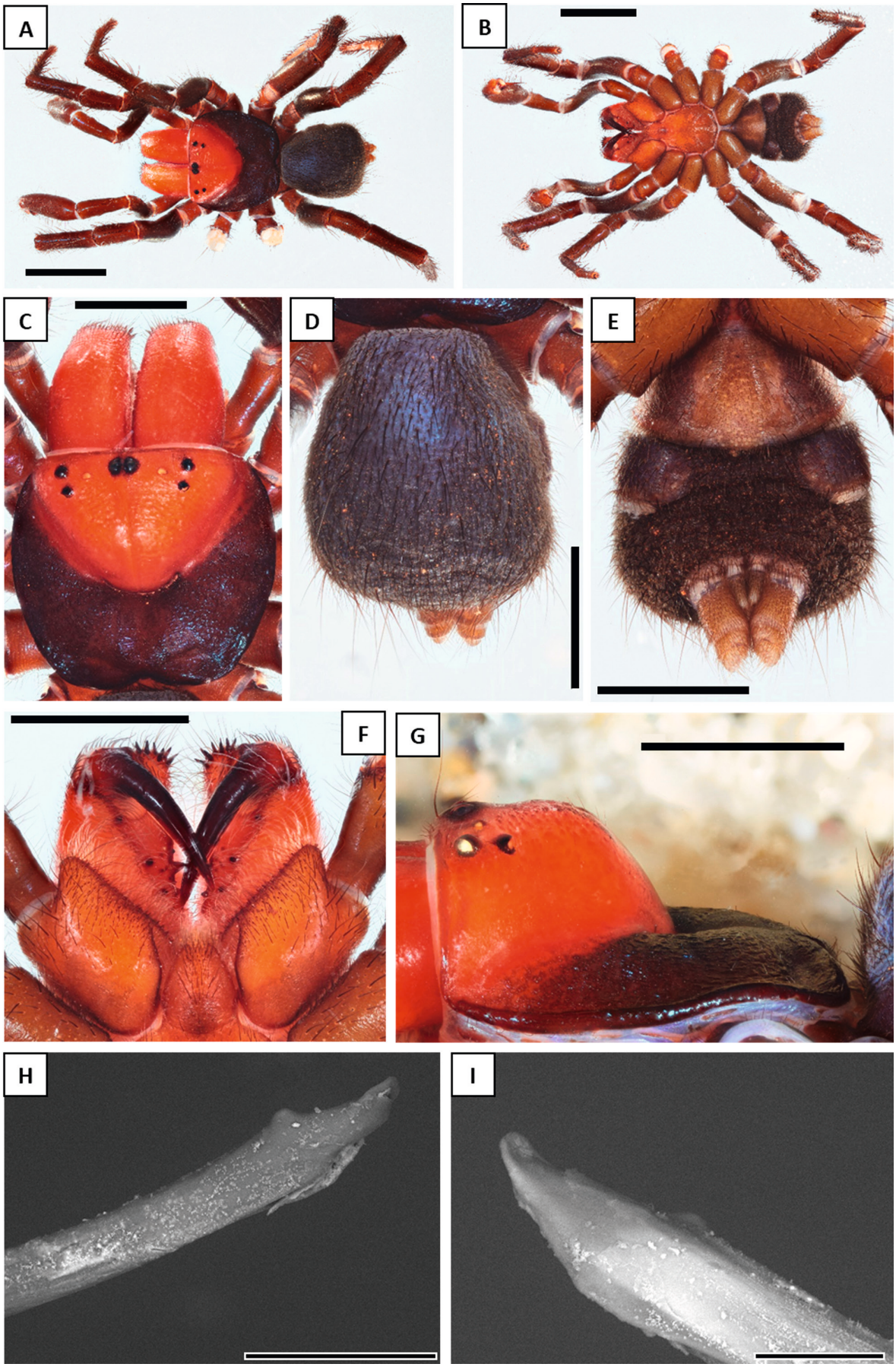

Figure 3. *Missulena davidi* sp. nov. Male holotype (WAMT119725): **A** habitus, dorsal view; **B** same, ventral view; **C** carapace, dorsal view; **D** abdomen, dorsal view; **E** same, ventral view; **F** maxillae, labium, and chelicerae, ventral view; **G** carapace, lateral view. Male paratype (WAMT119727), left pedipalp, **H** embolus with embolar tooth, prolateral view; **I** same, retrolateral view. Scale bars: A, B 4.0 mm; C–G 2.0 mm; H 100 µm; I 40 µm.

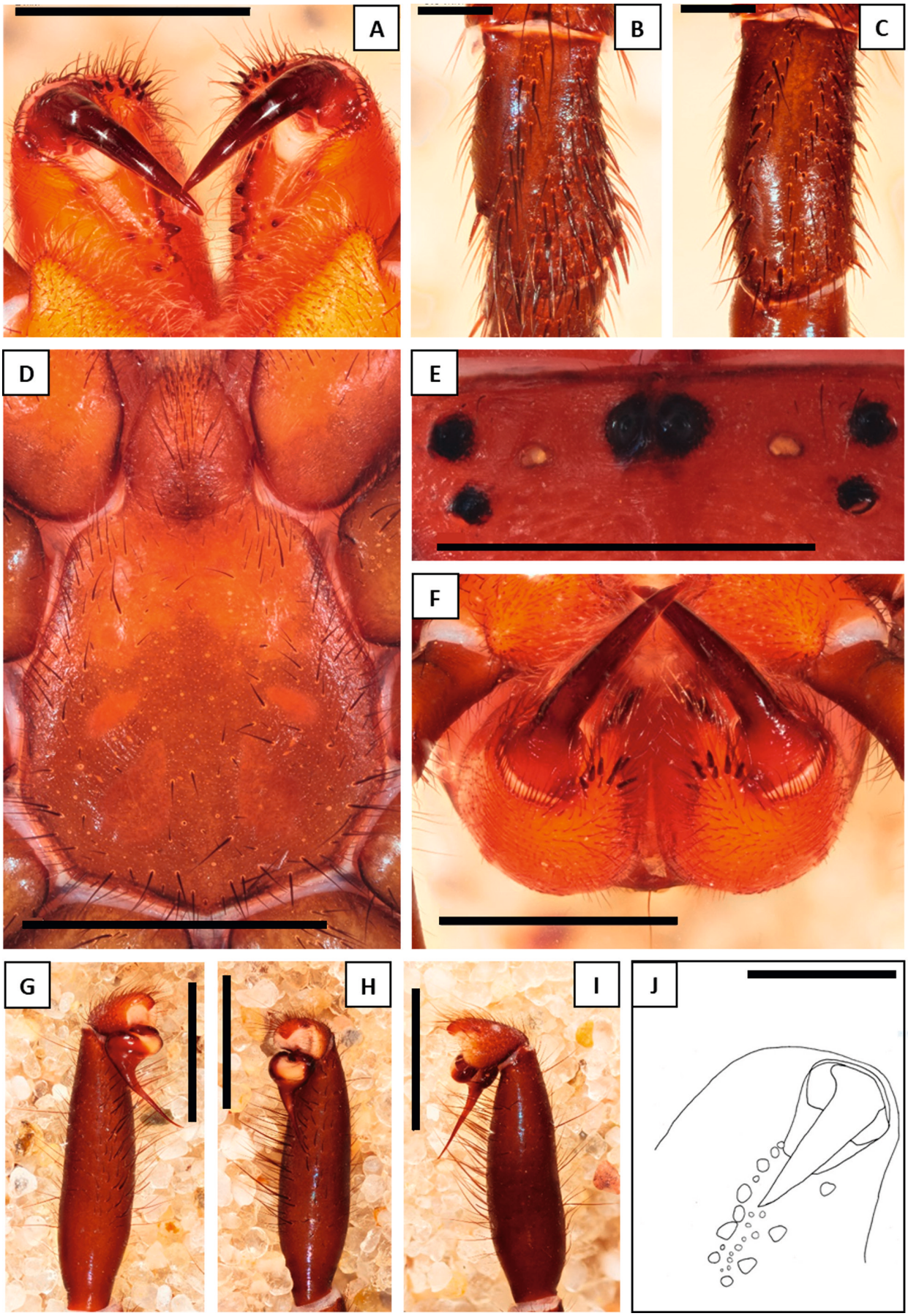

Figure 4. *Missulena davidi* sp. nov. Male holotype (WAMT119725): **A** chelicerae with cheliceral groove, ventral view; **B** patella III, dorsal view; **C** patella IV, dorsal view; **D** sternum, ventral view; **E** eye region, dorsal view; **F** rastellum, frontal view; **G** right pedipalp, retrolateral view; **H** same, ventral view; **I** same, prolateral view; **J** pattern of cheliceral teeth in cheliceral groove. Scale bars: A, D–H 2.0 mm; B, C 0.5 mm; J 1.0 mm.

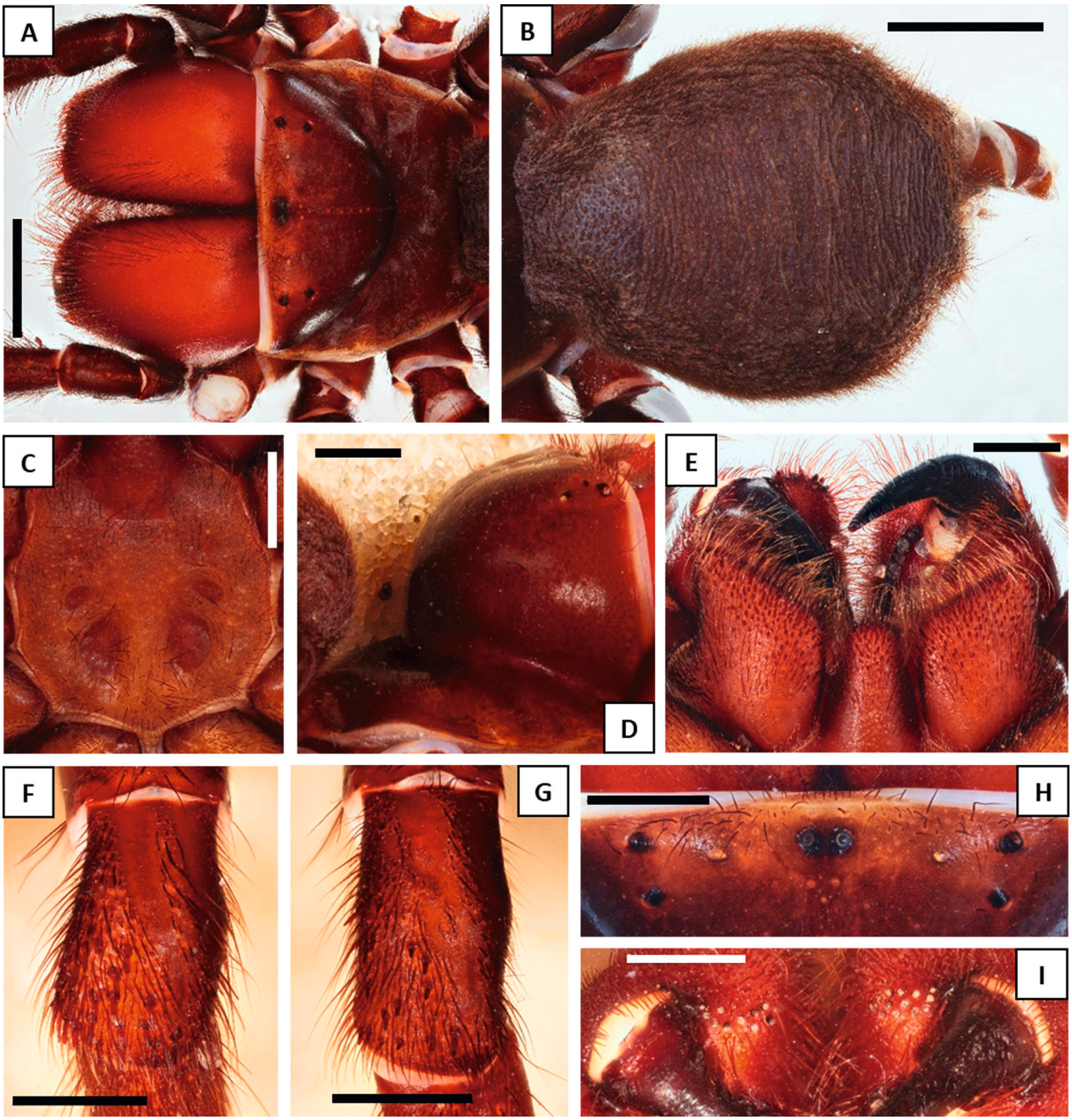

Figure 5. *Missulena davidi* sp. nov. Female allotype (WAMT107393): **A** carapace, dorsal view; **B** abdomen, dorsal view; **C** sternum, ventral view; **D** carapace, lateral view; **E** maxillae, labium and chelicerae, ventral view; **F** patella III, dorsal view; **G** patella IV, dorsal view; **H** eye region, dorsal view; **I** rastellum, frontal view. Scale bars: A, B 4.0 mm; C–I 2.0 mm.

slightly depressed. **Abdomen**: 3.88 long and 3.4 wide; shape of a rounded trapezoid (Fig. 3D); 4 spinnerets, PLS 1.12 long, 0.48 wide; PMS 0.43 long, 0.23 wide. **Pedipalp**: length of trochanter 1.49, femur 3.68, patella 1.68, tibia 4.01, tarsus 0.72; all segments with setae, tibia ventrally covered with comparably long setae (Fig. 4I); tibia rather thin and slightly recurved, 1.00 wide on the widest point from dorsal and prolateral view (Fig. 4G–I); bulb roughly pyriform (Fig. 4G–I), two strongly sclerotized sections connected by a velar median structure ("haematodocha"); embolus short with an intumescence in proximal region; tip of embolus triangular with a small lamella and a tooth best visible from prolateral view (paratype, Fig. 3H, I). **Legs**: brown setae of various sizes on all sides of the legs and bent strongly towards the exterior with the exceptions of some long, dorsal setae on tibia I and IV; ventral preening comb on tarsi and metatarsi III and IV. **Leg spination**: leg I: tibia rv0, v5, pl0, d0; metatarsus rv3, v8, pl2, d0; tarsus rv3, v3, pl4, d0; leg II: tibia rv0, v8, pl0, d0; metatarsus rv0, v11, pl0, d0; tarsus rv3, v3, pl2, d0; leg III: tibia rv4, v8, pl0, d11; metatarsus rv4, v11, pl0, d11; tarsus rv5, v9, pl4, d5; leg IV: tibia rv0, v5, pl0, d0; metatarsus rv0, v16, pl0, d2; tarsus rv4, v10, pl3, d3; patella I with one spine prolateral close to the tibia and patella II with one spine ventrally also close to the tibia; patella III with ca. 23 spines prolateral to dorsal (Fig. 4B), 1 spine retrolateral; patella IV with one spine dorsal close to the tibia and approx. 12 small spines (Fig.

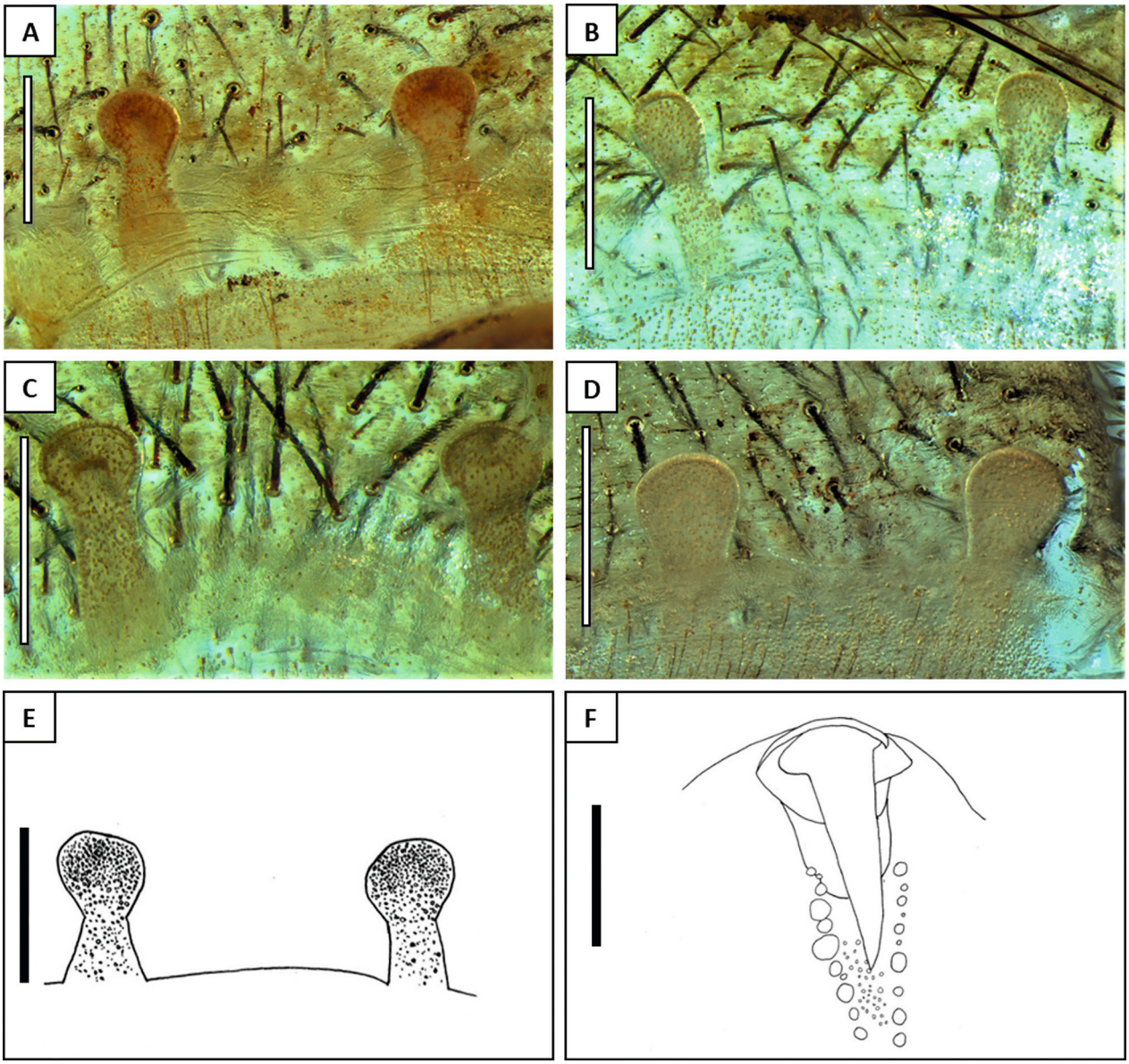

Figure 6. *Missulena davidi* sp. nov. Variability of spermatheca in females: **A** allotype specimen WAMT107393, clade I; **B** specimen WAMT119995, clade IV; **C** specimen WAMT126272, clade II; **D** specimen WAMT122226, clade III. Systematic drawings based on allotype WAMT107393: **E** spermatheca; **F** pattern of cheliceral teeth in the cheliceral groove. Scale bars: A–E 0.5 mm; F 2.0 mm

4C) and ca. 18 prolateral, also very small. **Leg measurements**: Leg I: femur 3.72, patella 1.29, tibia 2.72, metatarsus 2.37, tarsus 1.37, total 11.47. Leg II: femur 3.31, patella 1.36, tibia 2.43, metatarsus 2.26, tarsus 1.38, total 10.74. Leg III: femur 2.72, patella 1.26, tibia 1.93, metatarsus 1.92, tarsus 1.35, total 9.18. Leg IV: femur 3.45, patella 1.47, tibia 2.76, metatarsus 2.41, tarsus 1.51, total 11.6. Formula: 4>1>2>3.

FEMALE (based on allotype; WAM T107393). Total length 23.9. **Colour**: Carapace brown (Fig. 5A); chelicerae reddish-orangish with a darker spot (dark reddish-brown) on each chelicerae base (Fig. 5A); eye region light reddish colour similar to chelicerae (Fig. 5A); abdomen greyish-brown with a faint, dorsal, metallic blue sheen (Fig. 5B); sternum light brown fading into a reddish-brown towards labium (Fig. 5C), sigilla darker brown (Fig. 5C); labium und maxillae reddish-brown (Fig. 5E); legs brown (Fig. 5F, G); spinnerets lighter brown (Fig. 5B). **Carapace**: 7.31 long and 9.88 wide; clypeus 0.74; pars cephalica covers 4.72 of its length, is highly elevated and smooth (Fig. 5D) with some setae going along the margin of the chelicerae as well as vertically in a line from the AME to fovea plus some random setae (Fig. 5A); pars thoracica smooth surface with bands of faint, radial fissures (Fig. 5A). **Eyes**: OQ 4.9 times wider than long; width of each eye pair AME 0.91, APE 6.01, PME 3.59 and PLE 5.54; diameter of AME 0.33, ALE 0.36, PME 0.25, PLE 0.3; anterior eyes in one straight line; posterior eyes clearly recurved (Fig. 5H). **Chelicerae**: 5.65 long and 4.15 wide on the base; edges rounded and recurved with the widest point being 4.73 close to the chelicerae base (Fig. 5A); long setae along the inner margin increasing in amount towards rastellum; short and fewer setae along the outer margin and no setae in centre (Fig. 5A); rastellum present with 10–14 conical spines on each chelicera and long, densely disordered se-

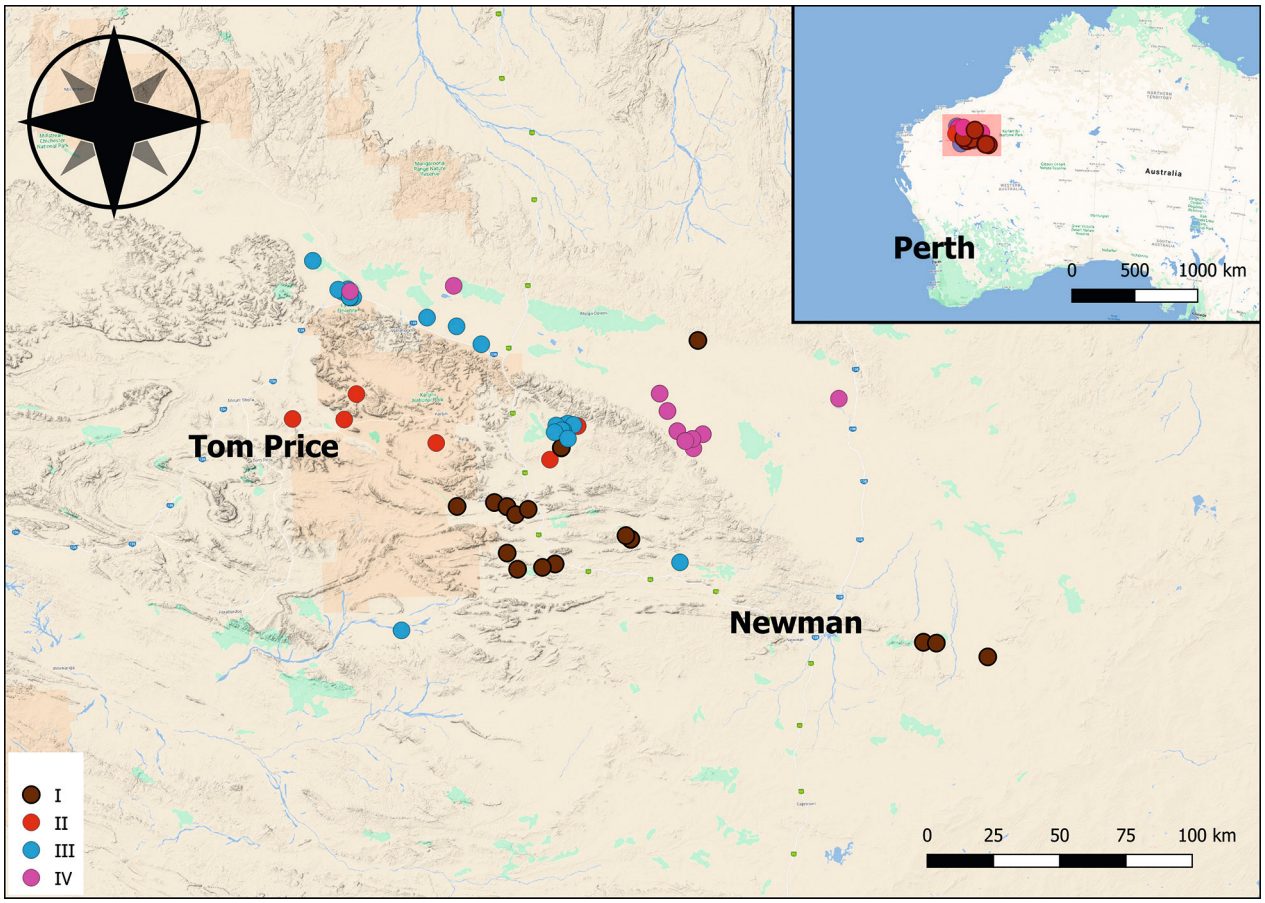

Figure 7. Distribution records of the *Missulena davidi* sp. nov. in the Pilbara in Western Australia, marked with colour according to clades of the phylogenetic tree (Fig. 2).

tae (Fig. 5I); approx. 25 setae cover anterior base of fang; inner margin of cheliceral furrow with two main rows of cheliceral teeth and a small cheliceral teeth area in between (Fig. 6F); prolateral row with 11 teeth, the first 3 teeth next to the fang's base are partially grown together; retrolateral row with 10 teeth; intermediate area with approx. 32 small teeth. **Maxillae**: 4.48 long and 3.67 wide; at least 150–170 strongly developed cuspules along entire anterior margin (Fig. 5E). **Labium**: 4 long and 2.27 wide on the base; conical; at least 60 cuspules (Fig 5E); anterior pair of sigilla reach labiosternal junction; labiosternal junction clearly developed (Fig. 5C). **Sternum**: 6.32 long and 5.7 wide; oval (Fig. 5C); setae of various length somewhat densely but disordered along the margin and a similar amount of setae of various sizes spread evenly over the sternum; 4 pairs of sigilla, anterior pair small and hardly visible, second pair (anterior-posterior) smallest and divided in circles, third pair larger than second and roughly in the shape of an elongated oval, and posterior pair biggest (roughly 4 times the size of the third pair); all sigilla depressed, two anterior pairs just slightly, two posterior pairs strongly. **Abdomen**: 10.87 long and 9.12 wide; surface covered with horizontal wrinkles and dense setae (Fig. 5B); PLS 2.84 long and 1.5 wide; PMS 1.43 long and 0.6 wide. **Pedipalp**: Length of trochanter 1.5, femur 4.62, patella 1.79, tibia 3.23, tarsus 2.96; approx. 17 spines spread prolateral, retrolateral and ventral on tarsus. **Genitalia**: one pair of simple and rounded spermathecae, sperm ducts relatively short (Fig. 6A–E). **Legs**: densely covered in brown setae of various sizes on all sides of the legs and bent towards the exterior with the exceptions of some long, dorsal setae on tibia, metatarsus and tarsus. **Leg spination**: leg I: tibia rv0, v0, pl0, d0; metatarsus rv1, v2, pl0, d0; tarsus rv6, v13, pl6, d0; leg II: tibia rv0, v0, pl0, d0; metatarsus rv1, v3, pl0, d0; tarsus rv6, v11, pl3, d0; leg III: tibia rv1, v0, pl2, d8; metatarsus rv0, v1, pl0, d18; tarsus rv7, v11, pl7, d6; leg IV: tibia rv0, v0, pl1, d5; metatarsus rv0, v3, pl4, d2; tarsus rv1, v15, pl9, d3; patellae I and II aspinose; patella III with ca. 28 spines prolateral to dorsal (Fig. 5F); patella IV with ca. 18 spines prolateral to dorsal (Fig. 5G). **Leg measurement**: leg I: femur 5.2, patella 2.16, tibia 3.4, metatarsus 2.5, tarsus 1.93, total 15.19. leg II: femur 5.32, patella 2.54, tibia 3.02, metatarsus 2.86, tarsus 2.04, total 15.78. leg III: femur 5.03, patella 2.64, tibia 2.39, metatarsus 3.08, tarsus 2.15, total 15.29. leg IV: femur 5.6, patella 2.61, tibia 3.66, metatarsus 3.31, tarsus 2.24, total 17.42. Formula: 4>2>3>1.

Etymology. The specific epithet is a patronym in honour of the senior author's husband, David A. Greenberg.

Distribution. Pilbara region of Western Australia, excluding the northern Pilbara subregion, extending into the Little Sandy Desert region. The known linear range of this species is 295 km (Fig. 7).

Table 1. Summary of scored characters in *M. davidi* sp. nov., *M. manningensis* sp. nov. and *M. iugum* sp. nov.. M = Median, n = sample size.

Characters	*M. davidi*–**males (n = 12)**				*M. davidi*–**females (n = 26)**					*M. manningensis* **(n = 1)**	*M. iugum* **(n = 2)**
	Clades			**All clades combined**	**Clades**				**All clades combined**		
	I (n = 4)	**II (n = 4)**	**III (n = 4)**		**I (n = 10)**	**II (n = 7)**	**III (n = 7)**	**IV (n = 5)**			
Carapace length [mm]	3.86–4.2	3.95–4.74	3.58–4.11	3.58–4.74 M: 4.03	5.19–8.55	5.12–8.54	6.75–8.59	6.21–8.76	5.12–8.97 M: 7.91	3.6	3.68–3.87
Carapace width [mm]	4.67–4.96	4.56–5.55	4.23–4.88	4.23–5.55 M: 4.77	6.28–10.7	6.71–10.44	8.39–12	8.14–10.85	6.28–12 M: 10.28	4.61	4.57–4.98
Carapace height [mm]	1.73–2.54	1.92–2.24	1.75–2.31	1.73–2.54 M: 2.16	Not measured					1.96	1.67–1.69
Pars cephalica ratio to carapace (in %)	63.4–64.5	63.2–67.3	62.0–64.8	62–67% M: 64%	62.6–70.3	65.6–74.6	61.2–71.9	62.5–73.4	61–75% M: 67%	63%	60-62%
PLE ratio to ALE (in %)	90.5–98.2	89.7–95.4	92.4–96.0	90–98% M: 94%	84.3–93.0	84.6–90.4	86.1–94.3	85.5–94.7	84–95% M: 90%	95%	87–90%
PME ratio to ALE (in %)	60.7–64.5	59.6–62.9	59.0–64.1	59–64% M: 62%	57.0–67.8	55.7–60.6	52.2–65.0	56.9–65.9	52–68% M: 60%	64%	65–69%
Cuspules right maxillae	50–80	55–60	50–90	50–90 M: 60	75–200	130–180	120–230	130 -200	75–230 M: 170	30	70–100
Cuspules left maxillae	45–70	55–80	35–70	35–80 M: 60	80–190	110–160	120–220	90–150	80–220 M: 150	30	70–85
Cuspules labium	25–30	15–25	20–30	15–40 M: 25	35–65	30–55	35–100	25–65	25–100 M: 48	5	30–35
Ridge in the Cheliceral groove	Not present				Not present					Not present	Present
Right rastellum	5–8	4–9	5–8	4–9 M: 6	8–15	11–17	7–18	5–12	5–18 M: 12	5	8
Left rastellum	4–8	5–10	6–9	4–10 M: 8	7–19	11–17	4–16	7–15	4–19 M: 12	8	8–9
Spination 1st patella	Not individually measured			rl: 0; v: 0–1; pl: 1–7; d: 0	Not individually measured				rl: 0; v: 0; pl: 0; d: 0	rl: 0; v: 1; pl: 8; d: 0	rl: 0; v: 3–9; pl: 9–12; d: 0
Spination 2nd patella				rl: 0; v: 1; pl: 0; d: 0					rl: 0; v: 0; pl: 0; d: 0	rl: 0; v: 1; pl: 1; d: 0	rl: 0; v: 2; pl: 0; d: 0
Spination 3rd patella				rl: 1–2; v: 0; pl/d: 23–25					rl: 0; v: 0; pl/d: 26–28	rl: 1; v: 0; pl/d: 26	rl: 4; v: 2–3; pl/d: 27
Supination 4th patella				rl: 0–1; v: 0; pl: 16–18; d: 1 + ~12 (small)					rl: 0; v: 0; pl/d: 17–26	rl: 0; v: 0; pl: 14 (small); d: 15 (small)	rl: 0; v: 3 (or just thickened setae); pl: 6 (small); d: 7 (small)

Genetic structure. The species is highly structured across its range with four genetic clades that have sympatric distributions (Figs 2, 7).

Remarks. This species had been labelled "MYG045" in previous barcoding studies (Castalanelli et al. 2014).

Variability. Assessment of 19 characters in male *M. davidi* sp. nov. and 18 characters in females (Table 1) highlights substantial variation in many characters within and between sampling localities, in both the male and female specimens examined.

In both sexes there is substantial variation in body colouration. In males, the chelicera and pars cephalica ranged from a bright red (specimen WAM T119729; Fig. 13A) to a red with a shade of orange (male: T120081; Fig. 13B) whereas abdominal colour in dorsal varied between green, purple and blue metallic tones to no metallic sheen at all (Fig. 13G–H). Colouration of the pars thoracica ranged from light brown (T119733) to nearly black (T119731) and the orange to olive transition on the sternum and coxa was also highly variable (compare T84005; Fig. 13F with T113596; Fig. 13E). In females, cheliceral colouration ranged between dark red (T116874; Fig. 14A) to a light orange (T119979 or T116776; Fig. 14B). The abdomen in some specimens had a metallic sheen and the sternum varied between uniformly orange (T116776; Fig. 14F) to a full transition from orange to dark red (T119711; Fig. 14G). Colour of legs and pars thoracica ranged between light brown (T116776) to dark brown (T125308). The colour variations still hold true if considering possible artefacts of preservation, i.e. varying trapping liquids, ethanol concentration during storage, and time of preservation.

Variability was also high in rastellum spination and cuspule counts. Some male specimens had about twice as many rastellum spines (Fig. 13L, M) and/or cuspules on both maxillae and labium than others. Female variability was even higher with some specimens having up to four times more maxillary cuspules (Fig. 14H, I) or nearly five times more spines on the rastellum (17; Fig. 14N, O) than others. The spination of the patellae was also variable which included spinal counts, size, and positioning of the individual spines. While male specimens showed variation on the first, third and fourth patella, females only had spines on the third and fourth patella (see Table 1 for details). The shape of the sternum in females varied considerably between ovoid and round, and the shape, size and position of the sternal sigilla differed substantially (Fig. 14F, G). The second pair of sigilla was subdivided into two depressions in some female specimens but not in others. Variation in body size was also substantial (Fig. 15) and the carapace length ranged from 3.58 to 4.74 in males and 5.12 to 8.97 in females.

Eye ratio of the PLE and PME pair width in relation to the ALE pair width varied less than other characters. While still showing variation in males and females its range was less extreme (within 8% in males and 16% in females) than in other characters (Figs 13I–K, 14J–M; see boxplot Fig. 16). Male bulb structure also varied little (Fig. 3 H, I).

There was no correlation between geographical distance of samples and morphological divergence. For example, two females of the clade III (WAM T126260 and T126264) from one locality showed substantial differences in the number of rastellum spines (9 vs 17 respectively), which was also notable for four male specimens of the clades II and III (T119726–T119729) from the same location (4 to 10 spines). Similar results were inferred for cuspule count in these males (55 to 80 cuspules on the maxillae).

3.2. *Missulena iugum* sp. nov.

http://zoobank.org/D846D8BD-F6FB-4E8E-8C16-BA6574CF-0F11

Figs 8–10

Type material. Holotype: AUSTRALIA – Western Australia • ♂; Mt Ida, 80 km NW of Menzies; 29°12.5′S 120°24.48′E; 29 Mar. 2012; V. Saffer leg.; pitfall trap; WAM T123110. **Paratype**: AUSTRALIA – Western Australia • ♂; same data as for holotype; 29°12.97′S 120°25.43′E; 27 July 2008; M. Quinn and G. Murray leg.; pitfall trap; WAM T110243.

Diagnosis. Males of *Missulena iugum* sp. nov. share the red chelicerae and pars cephalica with *M. davidi* sp. nov., *M. manningensis* sp. nov., *M. langlandsi*, *M. occataria* and *M. insignis* that are morphologically most similar. They differ from *M. langlandsi* by a longer carapace (>3.00 mm; *M. langlandsi* up to 2.8 mm) and a rastellum with strong, conical spines (simple in *M. langlandsi*). Rastellum and cuspules on labium and maxillae stronger than in *M. insignis* (rastellum: 8–9 spines; *M. insignis* 2–5; cuspules: *M. insignis* none). Pars cephalica lower than in *M. occatoria* (up to 1.69; *M. occataria* approx. 3.0) and carapace shorter (3.87 long, 4.98 wide; *M. occataria* approx. 5.0 long, 7.0 wide). Differs from *M. davidi* sp. nov. and *M. manningensis* sp. nov. by the presence of a ridge in the cheliceral groove (Fig. 9G, I).

Description. MALE (based on holotype; WAM T123110). Total length 9.89. **Colour**: pars cephalica and chelicerae orange (Fig. 8C); a slim, black ring surrounding the PME (Fig. 8G); pars thoracica brown with a light, metallic blue sheen (Fig. 8C); abdomen greyish with a very strong, metallic blue and green sheen on the dorsal side (Fig. 8D), ventrally more brownish with a faint hint of purple (Fig. 8E); sternum orange, slightly fading into olive with 8 sigilla in different shades of orange (Fig. 9C); labium and maxillae orange with a slightly darker reddish-orange spot on the base of labium (Fig. 8F); legs olive fading into light brown ventrally, dorsally brown (Fig. 8A–B); spinnerets beige-coloured (Fig. 8E). **Carapace**: 3.87 long, 4.98 wide and 1.67 high; clypeus 0.34; pars cephalica covers 2.34 of its length, is highly elevated and faintly granulated with very few setae (Fig. 9H); pars thoracica also granulated with bands of faint, radial fissures and with two notches close to the abdomen (Fig. 8C).

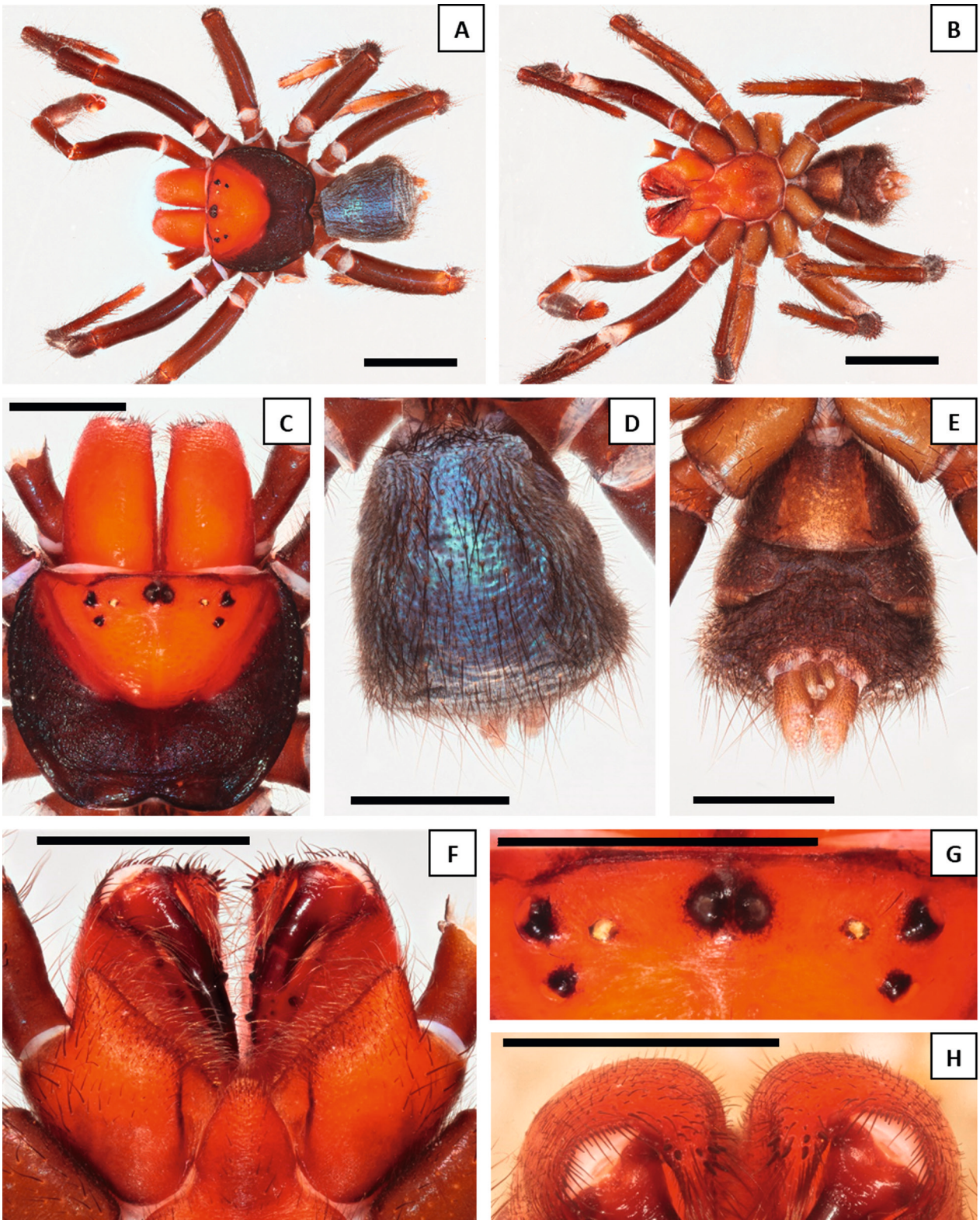

Figure 8. *Missulena iugum* sp. nov. Male holotype (WAMT123110): **A** habitus, dorsal view; **B** ventral view; **C** carapace, dorsal view; **D** abdomen, dorsal view; **E** same, ventral view; **F** maxillae, labium, and chelicerae, ventral view; **G** eye region, dorsal view; **H** rastellum, anterior view. Scale bars: A, B 4.0 mm; C–H 2.0 mm.

Eyes: OQ 3.7 times wider than long; outer width of each eye pair AME 0.53, ALE 2.54, PME 1.66 and PLE 2.2; diameter of AME 0.2, ALE 0.21, PME 0.11, PLE 0.19; anterior eyes slightly recurved; posterior eyes strongly recurved (Fig. 8G). **Chelicerae**: 2.28 long and 1.55 wide on the base; edges rounded and curved with the widest point being 1.57 very close to the chelicerae base (Fig. 8C); few setae along the inner margin and slightly more evenly spread setae along the anterior part of the chelicerae; rastellum present, slightly pronounced, consisting of a sclerotized process with 8 strong, conical spines (Fig. 8H); approx. 20 setae cover the anterior base of fang of

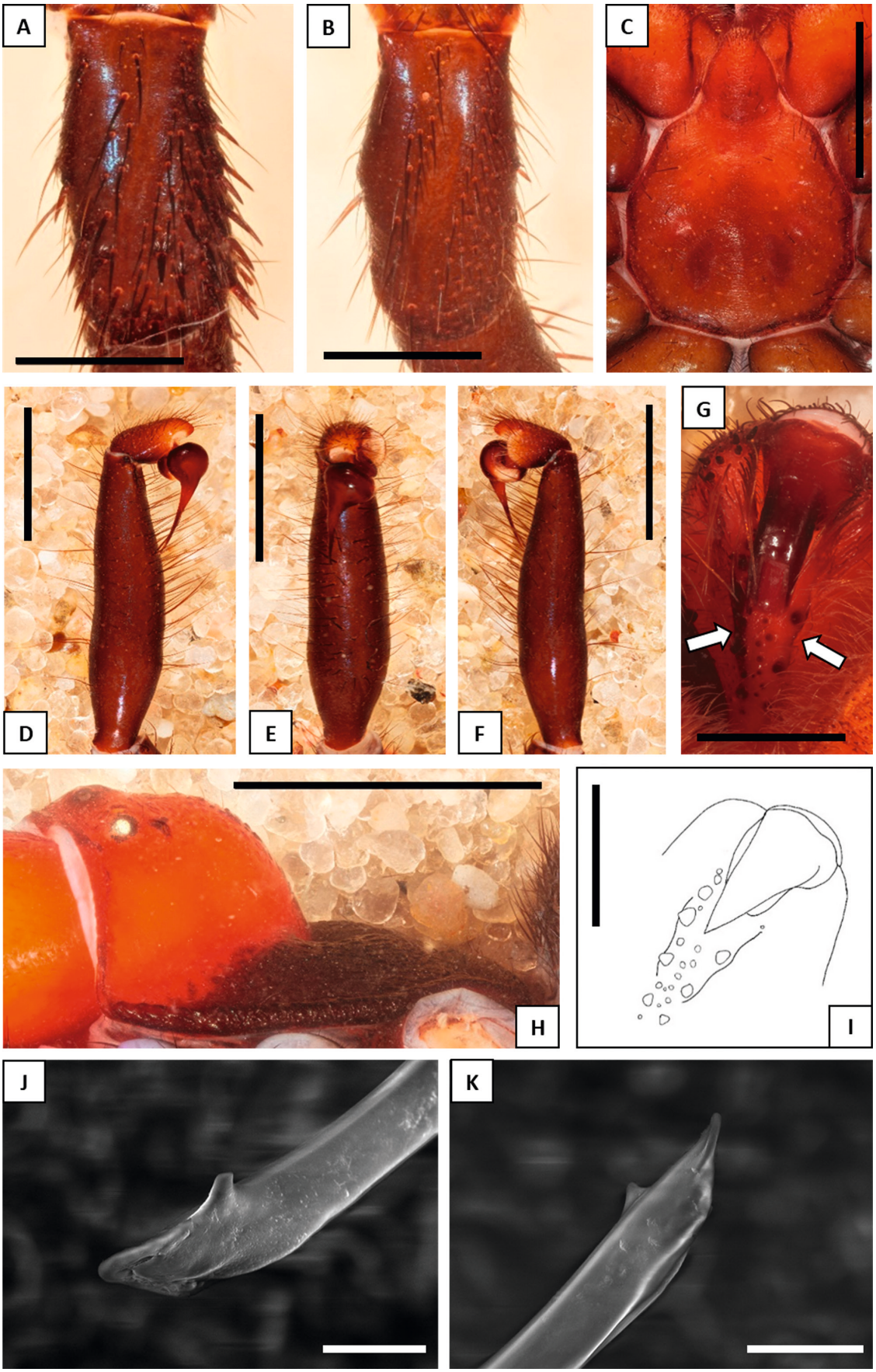

Figure 9. *Missulena iugum* sp. nov. Male holotype (WAMT123110): **A** patella III, dorsal view; **B** patella IV, dorsal view; **C** sternum, ventral view; **D** right pedipalp, retrolateral view; **E** same, ventral view; **F** same, prolateral view; **G** cheliceral teeth in cheliceral groove, arrows pointing to the ridge on both sides of the groove; **H** carapace, lateral view; **I** pattern of cheliceral teeth in cheliceral groove. Male paratype (WAMT110243), right pedipalp (left pedipalp not complete): **J** embolus with embolar tooth, prolateral-dorsal view; **K** embolus with lamella and tooth, retrolateral view. Scale bars: A, B, G, I 1.0 mm; C–F, H 2.0 mm; J 40 µm; K 50 µm.

each chelicera; inner margin of cheliceral furrow with 2 rows of teeth with each a ridge along the row and a general cheliceral teeth area in between those 2 clear rows (Fig. 9G, I); prolateral row with approx. 10 teeth; retrolateral row with 3 teeth (paratype has 4 teeth); intermediate area with 8 small teeth. **Maxillae**: 2.24 long and 1.52 wide; at least 85–100 weakly developed cuspules along entire anterior margin (Fig. 8F). **Labium**: 0.94 long and 0.91 wide on the base; conical; at least 35 weakly developed cuspules anteriorly (Fig. 8F); labiosternal junction visible (Fig. 9C). **Sternum**: 2.84 long and 2.77 wide; ovoid (Fig. 9C); setae of various length somewhat densely but disordered along the margin and a smaller amount of setae spread unevenly over the sternum; 4 pairs of sigilla, anterior pair small and hardly visible, second pair smallest (roughly half the size of the first pair) and circular, third pair larger than first and second pair (roughly 2 times bigger than first pair) in the shape of a drop, and posterior pair biggest (roughly 2.5 times the size of the third pair) in the shape of an elongated drop, all sigilla slightly depressed. **Abdomen**: 3.7 long and 3.41 wide; shape of a rounded trapezoid (Fig. 8D); 4 spinnerets, PLS 0.88 long, 0.55 wide; PMS 0.45 long, 0.19 wide (Fig. 8E). **Pedipalp**: length of trochanter 1.37, femur 4.17, patella 1.88, tibia 4.22, tarsus 0.75; all segments with setae, tibia ventrally densely covered with comparably long setae (Fig. 9D–F); tibia rather thin and slightly recurved from lateral view, 1.00 wide on the widest point from prolateral and 1.08 from dorsal view (Fig. 9D–F); bulb roughly pyriform, two strongly sclerotized sections connected by a velar median structure ("haematodocha"); embolus rather short with an intumescence in proximal region; tip of embolus triangular with a small lamella and a tooth best visible from prolateral view (paratype, Fig. 9J, K). **Legs**: brown setae of various sizes on all sides of the legs and bent towards the exterior; some comparably long setae dorsally on most segments double the length of the other setae; ventral preening comb on tarsi and metatarsi III and IV. **Leg spination**: leg I: tibia rl1, v13, pl0, d0; metatarsus rl2, v10, pl1, d0; tarsus rl2, v7, pl5, d0; leg II: tibia rl1, v11, pl1, d0; metatarsus rl2, v11, pl0, d0; tarsus rl5, v9, pl1, d0; leg III: tibia rl6, v5, pl5, d6; metatarsus rl5, v7, pl5, d9; tarsus rl10, v9, pl2, d6; leg IV: tibia rl1, v10, pl1, d1; metatarsus rl1, v9, pl3, d2; tarsus rl14, v13, pl5, d5; patella I with 9 spines spread out prolaterally and three spine ventrally in a vertical row; patella II two spines ventrally in a vertical row; patella III with 27 spines spread out dorsally and prolaterally, 4 spines retrolaterally (Fig. 9A) and 3 spines ventrally in a vertical row; patella IV with approx. 7 spines on the dorsal side (Fig. 9B), approx. 6 spines on the prolateral side, all very small, and 3 spines ventrally in a vertical row. **Leg measurement**: Leg I: femur 4.2, patella 1.63, tibia 3.06, metatarsus 2.76, tarsus 1.58, total 13.23. Leg II: femur 3.47, patella 1.53, tibia 2.66, metatarsus 2.24, tarsus 1.48, total 11.38. Leg III: femur 3.07, patella 1.35, tibia 1.88, metatarsus 2.37, tarsus 1.52, total 10.19. Leg IV: femur 3.91, patella 1.59, tibia 2.99, metatarsus 2.78, tarsus 1.64, total 12.91. Formula: 1>4>2>3.

Etymology. The specific epithet is a Latin noun (*iugum* = ridge) in apposition, referring to the strongly developed ridges along the cheliceral groove of the males.

Distribution. Known only from the Mt Ida region approximately 16 km east of Ularring in the Goldfields region of Western Australia (Fig. 10). The habitat of the holotype comprises *Acacia* shrubland.

3.3. *Missulena manningensis* sp. nov.

http://zoobank.org/D847F421-25EA-4FA2-8989-38837493-CD19

Figs 10–12

Type material. Holotype: AUSTRALIA – Western Australia • ♂; Mt Manning area, site CR2; 30°27.95′S 119°58.02′E; 21 June 2008; J. Francesconi leg.; WAM T92071.

Diagnosis. Males share with *M. davidi* sp. nov., *M. iugum* sp. nov., *M. langlandsi*, *M. occatoria* and *M. insignis*, the closest morphological matches, the red colouration of the chelicerae and pars cephalica. They differ from *M. langlandsi* by a longer carapace (>3.00 mm; *M. langlandsi* up to 2.8 mm) and the presence of strong, conical spines of the rastellum (simple in *M. langlandsi*). They differ from *M. occataria* and *M. insignis* by the lack of spines ventrally on patellae III and IV (at the most 1 thickened seta). Pars cephalica lower than in *M. occataria* (up to 1.96; *M. occataria* approx. 3.0) and carapace shorter (3.6 long, 4.61 wide; *M. occataria* approx. 5.0 long, 7.0 wide). More cuspules on the labium and maxillae than in *M. insignis* but less than in *M. davidi* sp. nov. (*M. insignis*: none; *M. manningensis* sp. nov.: 5 at labium, 30 at maxillae; *M. davidi* sp. nov.: 15–10 at labium, 35–100 at maxillae). Lacks a ridged cheliceral groove which is present in *M. iugum* sp. nov.

Description. MALE (based on holotype; WAMT92071). Total length 8.95. **Colour**: pars cephalica and chelicerae orange (Fig. 11C); a slim, black ring surrounding the PME (Fig. 11H); pars thoracica brown with a light, purplish sheen (Fig. 11C); abdomen greyish with a light, metallic blue sheen on the dorsal side (Fig. 11D), ventrally more brownish with a faint hint of purple (Fig. 11E); sternum orange, slightly fading into olive with 8 sigilla in different shades of orange (Fig. 11G); labium and maxillae orange with a dark olive spot on the base of labium (Fig. 11F); legs olive fading into light brown ventrally, dorsally brown (Fig. 11A, B); spinnerets beige (Fig. 11E). **Carapace**: 3.6 long, 4.61 wide and 1.96 high; clypeus 0.31; pars cephalica covers 2.25 of its length, is highly elevated and slightly granulated with very few setae (Fig. 12D); pars thoracica also granulated with bands of faint, radial fissures and with two deeply expressed notches close to the abdomen (Fig. 11C). **Eyes**: OQ 3.4 times wider than long; outer width of each eye pair AME 0.48, ALE 2.26, PME 1.44 and PLE 2.14; diameter of

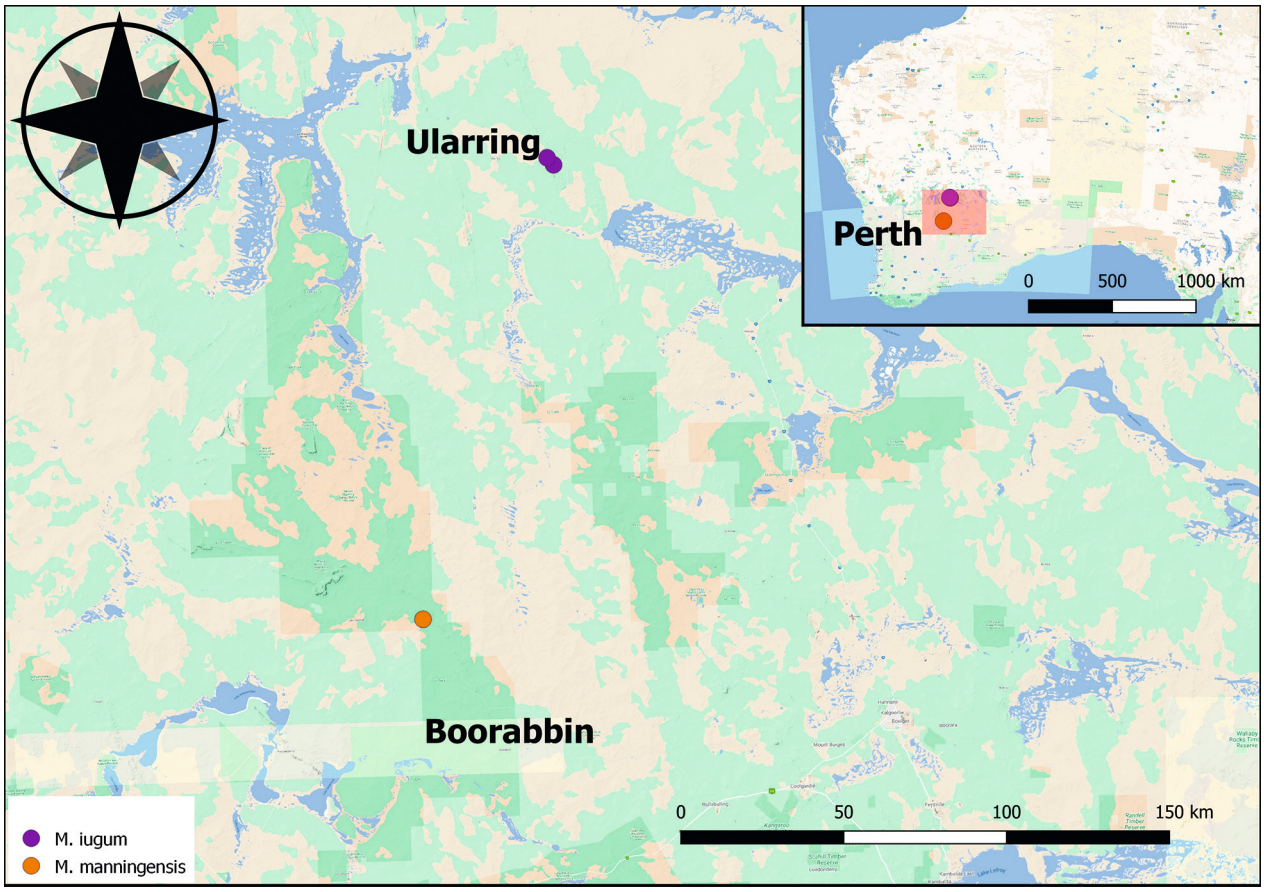

Figure 10. Distribution records of *Missulena manningensis* sp. nov. and *Missulena iugum* sp. nov. in Western Australia.

AME 0.19, ALE 0.19, PME 0.13, PLE 0.17; anterior eyes in a straight line; posterior eyes strongly recurved (Fig. 11H). **Chelicerae**: 2.17 long and 1.41 wide on the base; edges rounded and recurved with the widest point being 1.51 close to the chelicerae base (Fig. 11C); few setae along the inner margin and slightly more evenly spread setae along the anterior part of the chelicerae; rastellum present, slightly pronounced, consisting of a sclerotized process with 5 (left 8) strong, conical spines (Fig. 11I); over 20 setae cover the anterior base of fang of each chelicera; inner margin of cheliceral furrow with 2 rows of teeth and a general cheliceral teeth area in between those 2 clear rows (Fig. 12G); prolateral row with approx. 11 teeth; retrolateral row with 4 teeth; intermediate area with 5 small teeth. **Maxillae**: 2.09 long and 1.5 wide; at least 30 extremely weakly developed cuspules along anterior margin (Fig. 11F). **Labium**: 0.79 long and 0.86 wide on the base; conical; at least 5 extremely weak developed cuspules anteriorly (Fig. 11F); labiosternal junction visible (Fig. 11G). **Sternum**: 2.62 long and 2.29 wide; ovoid (Fig. 11G); setae of various length somewhat densely but irregular along the margin and a smaller amount of setae spread unevenly over the sternum; 4 pairs of sigilla, anterior pair very small and hardly visible, second pair also hardly visible, smallest of all pairs and divided into two circles, third pair significantly larger than second (roughly 4 times bigger) in the shape of an elongated oval, and posterior pair biggest (roughly 2 times the size of the third pair) and drop-shaped, all sigilla slightly depressed. **Abdomen**: 3.12 long and 2.74 wide; shape of a rounded trapezoid (but collapsed through preservation; Fig. 11D); 4 spinnerets, PLS 0.43 long (part of it broken off), 0.35 wide; PMS 0.37 long, 0.19 wide (Fig. 11E). **Pedipalp**: length of trochanter 1.64, femur 4.46, patella 1.82, tibia 3.75, tarsus 0.64; all segments with setae, tibia ventrally covered with comparably long and dense setae (Fig. 12A–C); tibia rather thin and slightly recurved, 1.00 wide on the widest point from dorsal/ventral and prolateral/retrolateral view (Fig. 12A–C); bulb roughly pyriform, two strongly sclerotized sections connected by a velar median structure (“haematodocha”); embolus rather short and bend with an intumescence in proximal region; tip of embolus triangular with a small lamella, best visible retrolateral (Fig. 12I), and a tooth, best visible prolateral (Fig. 12H). **Legs**: brown setae of various sizes on all sides of the legs and bent towards the exterior with the exception of the femur setae on ventral position which are mostly vertically; ventral preening comb on tarsi and metatarsi III and IV. **Leg spination**: leg I: tibia rl0, v17, pl0, d0; metatarsus rl0, v9, pl0, d0; tarsus rl0, v154-8-3, pl0, d0; leg II: tibia rl1, v12, pl0, d0; metatarsus rl0, v8, pl0, d0; tarsus rl0, v10, pl2, d0; leg III: tibia rl3, v13, pl0, d7; metatarsus rl3, v6, pl3, d9; tarsus rl3, v11, pl4, d5; leg IV: tibia rl0, v12, pl0, d0; metatarsus rl0, v12, pl5, d1; tarsus rl8, v13, pl7, d5; patella I with 8 spines spread out prolaterally and one spine ventrally close to tibia; patella II with one spine prolaterally and one ventrally both close to tibia; patella III with 26 spines

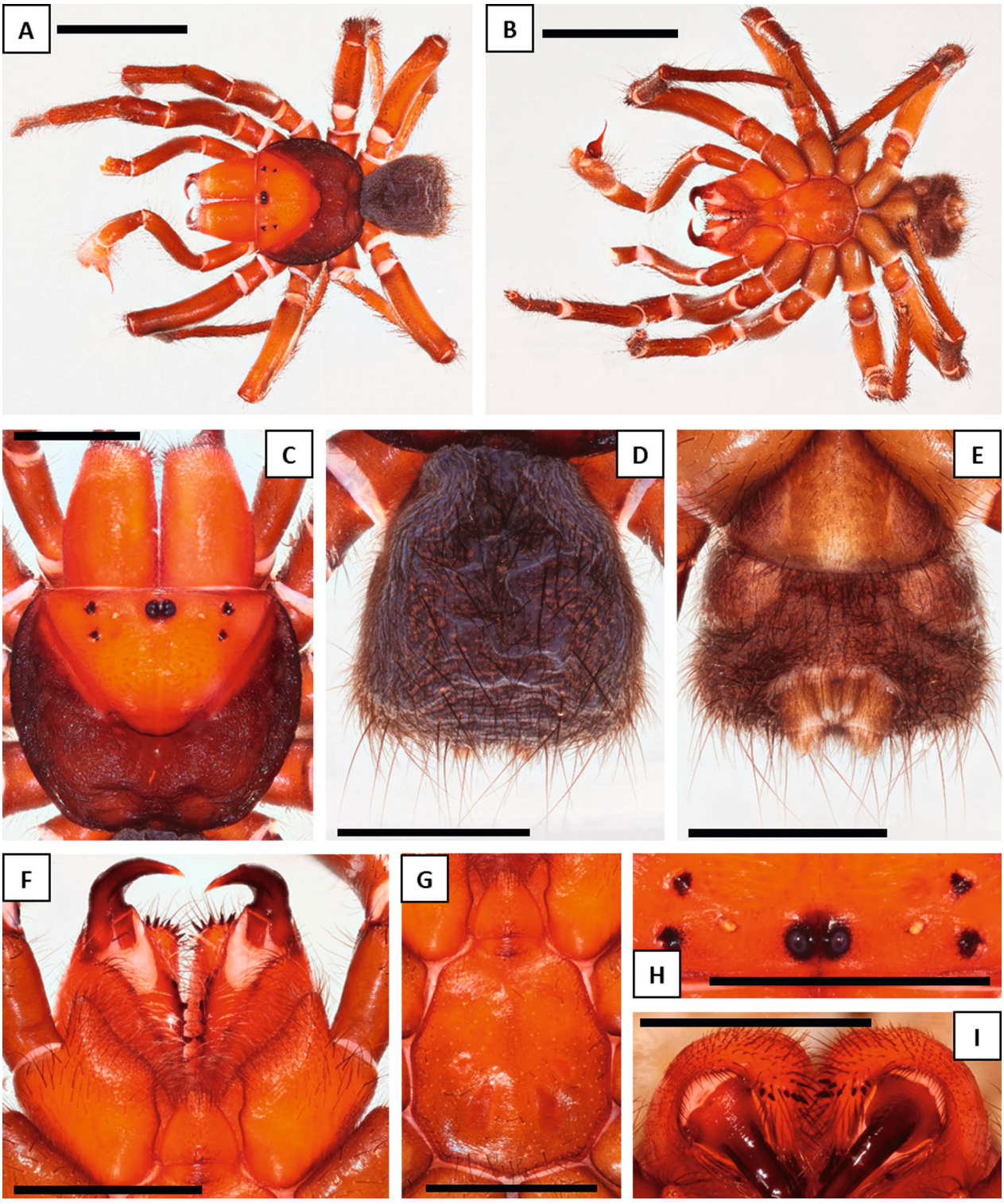

Figure 11. *Missulena manningensis* sp. nov. Male holotype (WAMT92071): **A** habitus, dorsal view; **B** same, ventral view; **C** carapace, dorsal view; **D** abdomen, dorsal view; **E** abdomen, ventral view; **F** maxillae, labium, and chelicerae, ventral view; **G** sternum, ventral view; **H** eye region, dorsal view; **I** rastellum, anterior view. Scale bars: A, B 5.0 mm; C–I 2.0 mm.

spread out dorsally and prolaterally and one spine retrolaterally (Fig. 12E); patella IV with approx. 14 spines on the dorsal side (Fig. 12F) and approx. 15 spines on the prolateral side, all very small. **Leg measurement**: Leg I: femur 4.0, patella 1.37, tibia 2.97, metatarsus 2.69, tarsus 1.56, total 12.59. Leg II: femur 3.4, patella 1.12, tibia 2.5, metatarsus 2.38, tarsus 1.47, total 10.87. Leg III: femur 2.81, patella 1.05, tibia 1.94, metatarsus 2.26, tarsus 1.54, total 9.6. Leg IV: femur 3.28, patella 1.13, tibia 2.83, metatarsus 2.41, tarsus 1.59, total 11.24. Formula: 1>4>2>3.

Etymology. The specific epithet refers to the type locality, Mt Manning, in the Goldfields region of Western Australia.

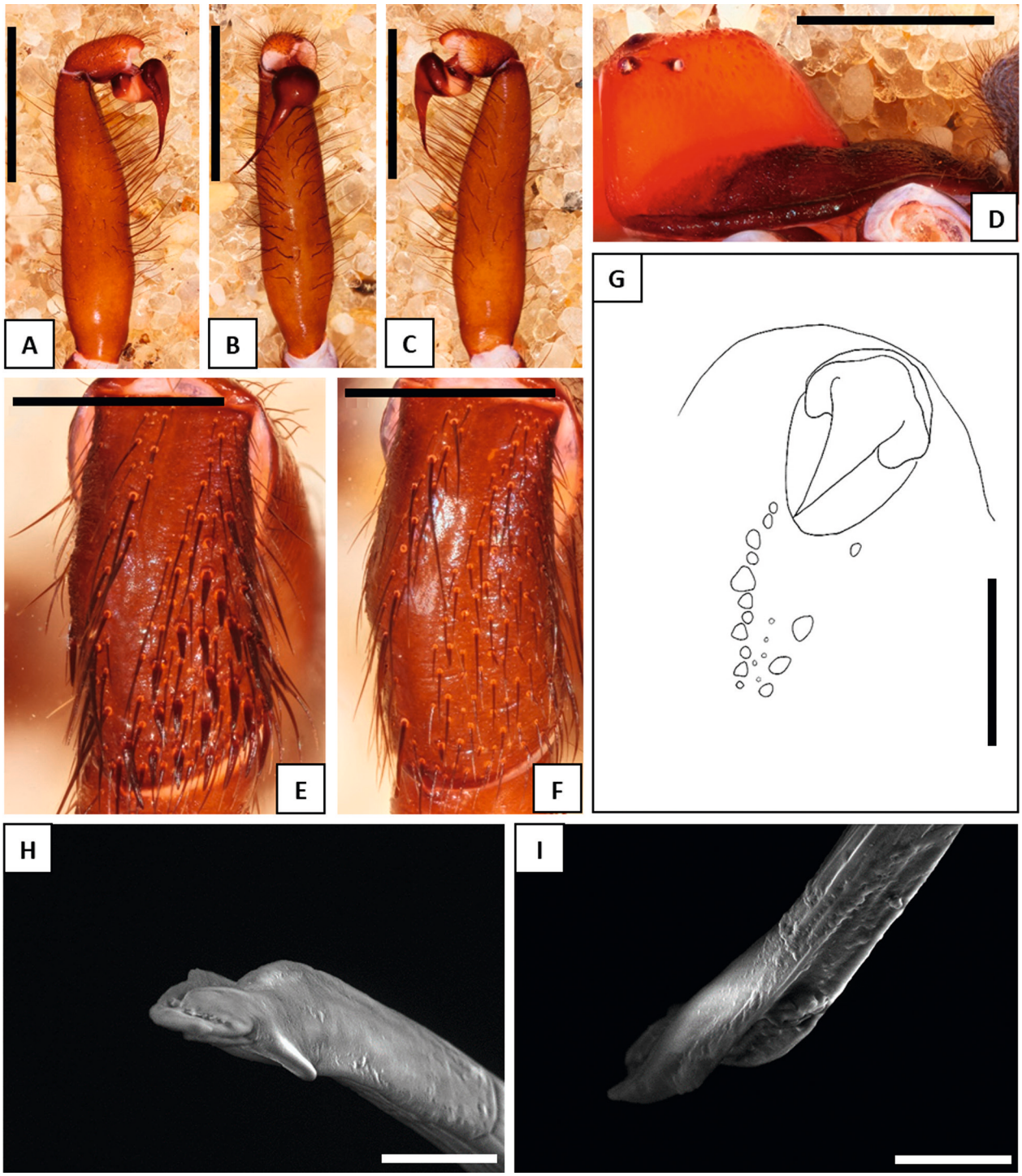

Figure 12. *Missulena manningensis* sp. nov. Male holotype (WAMT92071): **A** right pedipalp, retrolateral view; **B** ventral view; **C** prolateral view; **D** carapace, lateral view; **E** patella III, dorsal view; **F** patella IV, dorsal view; **G** pattern of cheliceral teeth in cheliceral groove; **H** left pedipalp, embolus with embolar tooth, prolateral-dorsal view; **I** left pedipalp, embolus with lamella, retrolateral-ventral view. Scale bars: A–D 2.0 mm; E–G 1.0 mm; H, I 40 µm

Distribution. Known only from the Mt Manning area approximately 47 km northwest of Boorabbin in the Goldfields region of Western Australia (Fig. 10). The habitat of the holotype comprises open tall eucalypt woodland with mixed shrubs.

4. Discussion

This study highlights the difficulty in diagnosing *Missulena* species morphologically in the absence of a molecular framework (e.g., a barcoding framework in our study). There clearly is substantial intraspecific variation if large specimen series are available for taxonomic descriptions,

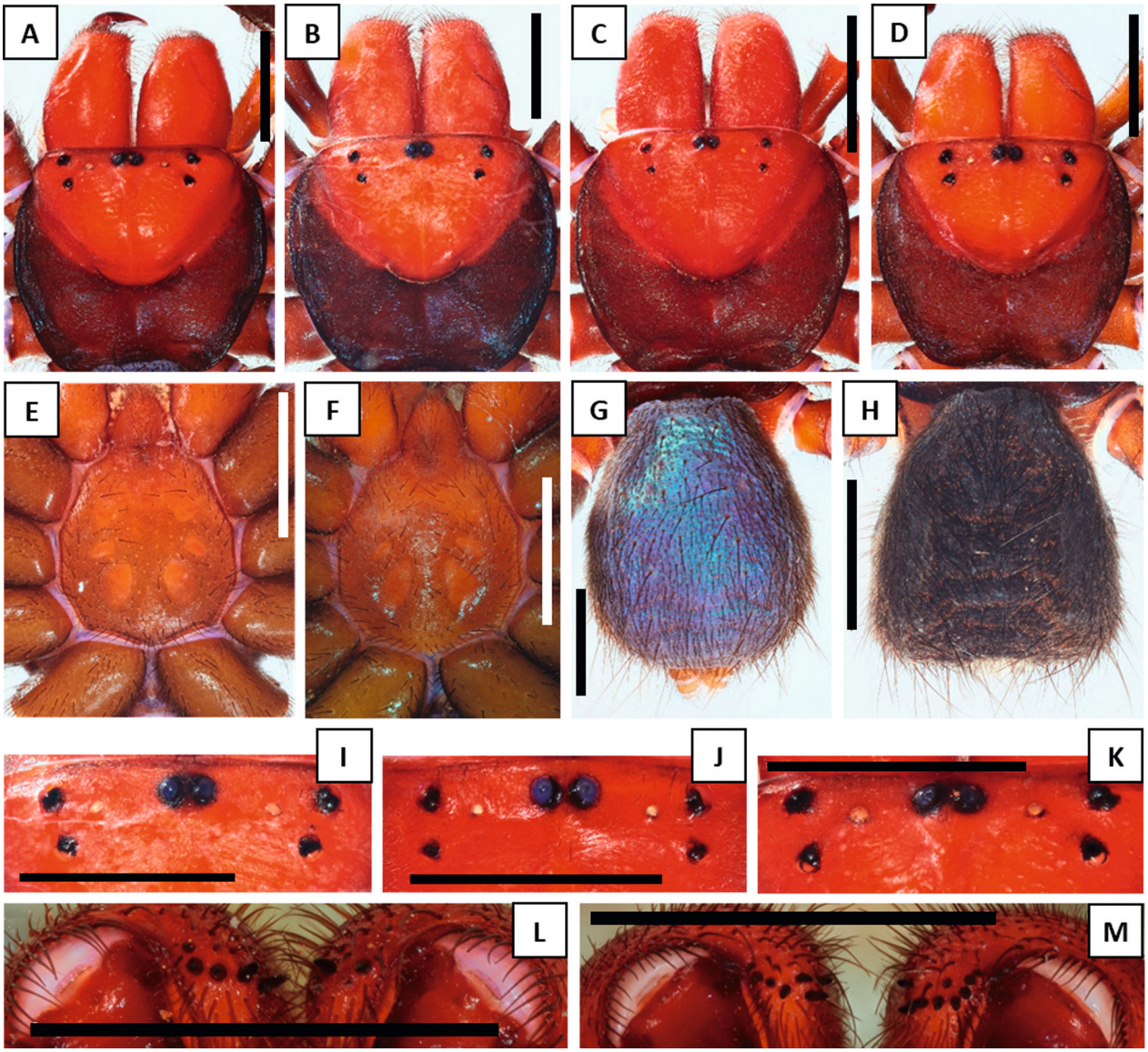

Figure 13. Variability in *Missulena davidi* sp. nov. males: **A** carapace, dorsal view (T119729, clade III); **B** carapace, dorsal view (T120081, clade II); **C** carapace, dorsal view (T119727, clade II); **D** carapace, dorsal view (T119733, clade III); **E** sternum, ventral view (T113596, clade I); **F** sternum, ventral view (T84005, clade I); **G** abdomen, dorsal view (T119727, clade II); **H** abdomen, dorsal view (T125176, clade III); **I** eye region, dorsal view (T120081, clade II); **J** eye region, dorsal view (T84005, clade I); **K** eye region, dorsal view (T119729, clade III); **L** rastellum, anterior view (T84005, clade I); **M** rastellum, anterior view (T119726, clade II). Scale bars: A–M 2.0 mm

but there also is morphological overlap in species that are clearly defined at the genetic level, as illustrated here by our species triplet that overlaps morphologically in several diagnostic characters (Figs 13–15; Table 1).

Our analyses suggest that females are substantially more variable than males, and that most of the morphological characters that are used in *Missulena* taxonomy are also variable. Characters that appear to be most useful in distinguishing species, at least in males, are the the number of cuspules on maxillae and labium, the positioning of eyes, specifically the PME and PLE width in relation to the ALE width, and the overall shape and colour of the carapace. Whilst variable and subject to overlap between species, the number of cuspules is a good character for our species triplet but perhaps also other *Missulena* species for which original data are available (e.g., Faulder 1995; Harms and Framenau 2013; Miglio et al. 2014; Framenau and Harms 2017). Eye patterns are also useful since their ratios can be quantified irrespective of carapace size. The width of the PME and PLE pair in relation to the ALE pair somehow overlaps in our species triplet, especially between *M. davidi* sp. nov. and *M. manningensis* sp. nov., but it does show a tendency and can be useful for other species in the genus, e.g., *M. faulderi* shows a smaller % width of PLE with ca. 78% vs. 90 to 98% in *M. davidi* sp. nov. (Harms and Framenau 2013).

Characters that we found to be highly variable and of little use, both within and between species, are body colouration (often subject to variable storage conditions), sternum size and shape, position and shape of sigilla (specifically variable in females), and the number of spines on the rastellum. This result is irrespective of potential

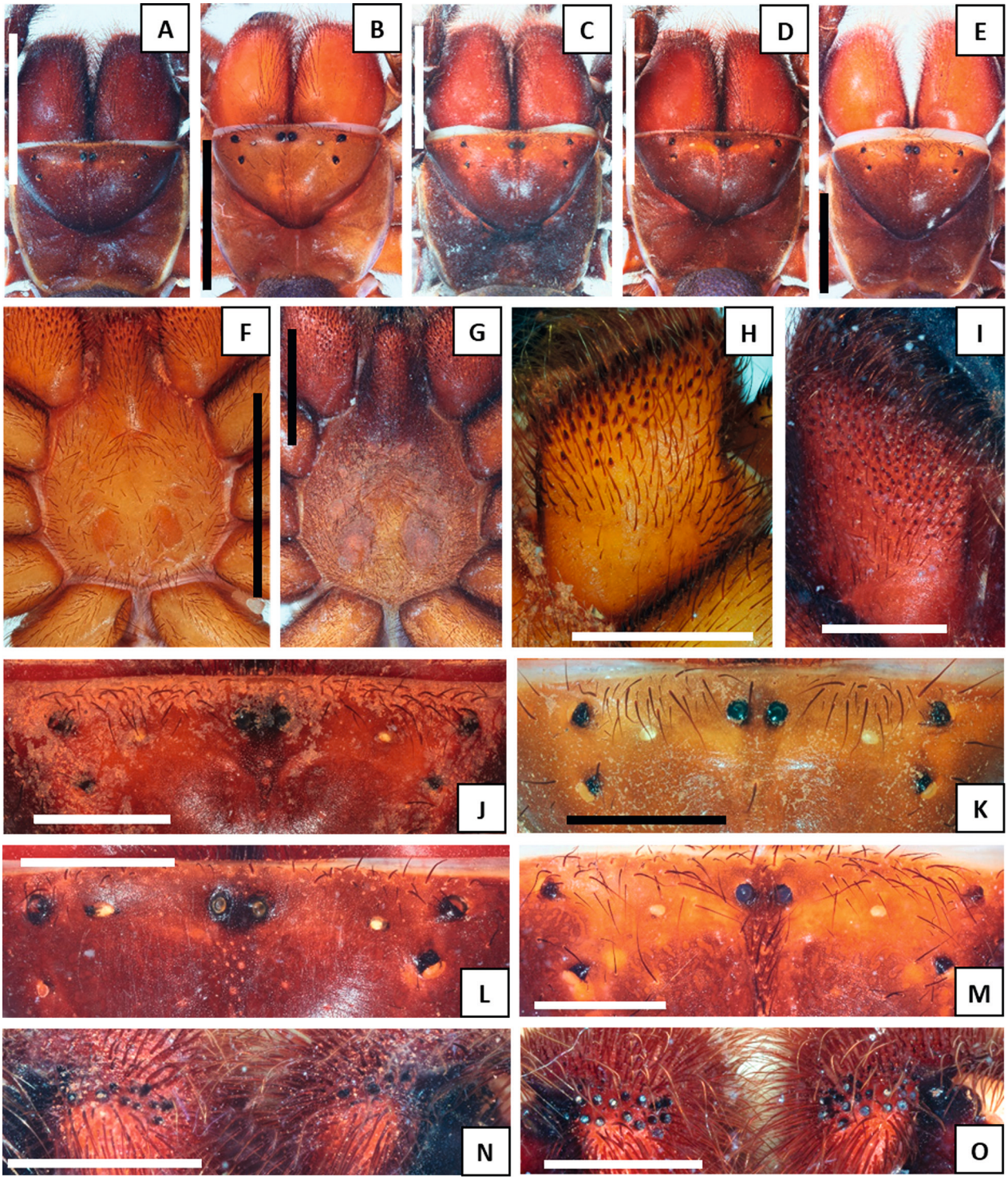

Figure 14. Variability in *Missulena davidi* sp. nov. females: **A** carapace, dorsal view (T116874, clade IV); **B** carapace, dorsal view (T116776, clade I); **C** carapace, dorsal view (T113591, clade III); **D** carapace, dorsal view (T122226, clade III); **E** carapace, dorsal view (T126272, clade II); **F** sternum, ventral view (T116776, clade I); **G** sternum, ventral view (T119711, clade I); **H** left maxilla, ventral view (T119979, clade IV); **I** right maxillae, ventral view (T116868, clade I); **J** eye region, dorsal view (T116839, clade I); **K** eye region, dorsal view (T119979, clade IV); **L** eye region, dorsal view (T122865, clade I); **M** eye region, dorsal view (T126264, clade III); **N** rastellum, anterior view (T125316, clade III); **O** rastellum, anterior view (T102165, clade I). Scale bars: A–G 4.0 mm; H–O 2.0 mm.

changes in the tree topology in the phylogeny if additional markers (e.g., nuclear genes) are used. A further character that should be treated with caution is the number and position of cheliceral teeth and a groove itself (e.g., ridge present in *M. iugum* sp. nov.; distal teeth blade in *M. faulderi*). For species delineation in females, we recommend evaluating patellae spination patterns further because there was little variability and the number of spines in *M. davidi* sp. nov. females (see Table 1) were different in comparison to other species for which data were

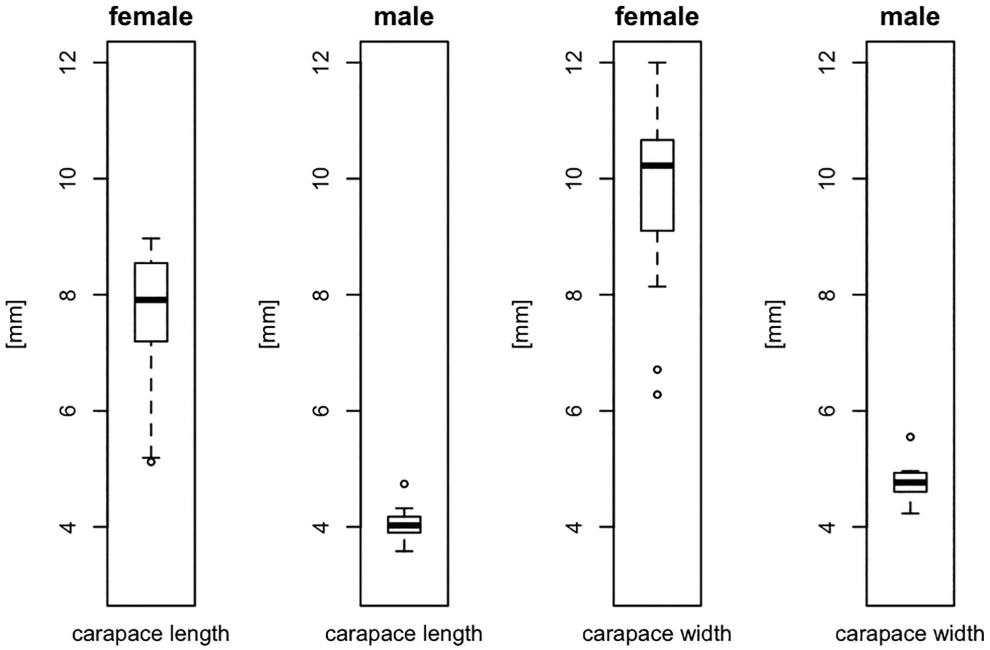

Figure 15. *Missulena davidi* sp. nov., male and female variability in carapace length and width in mm; n = 24 females, 12 males.

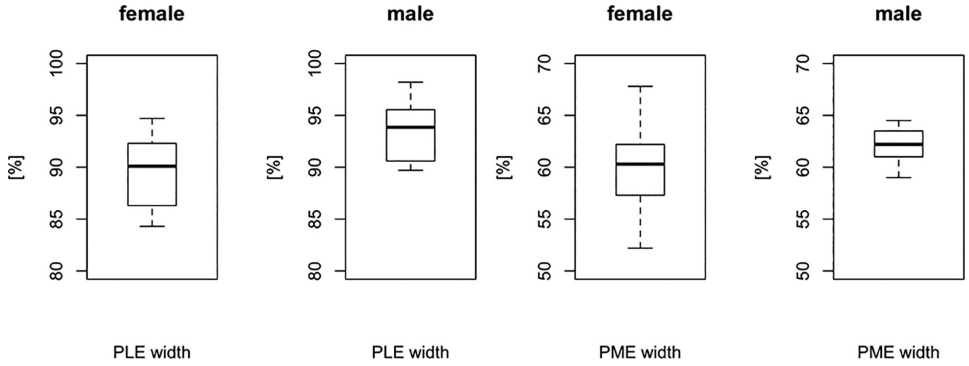

Figure 16. *Missulena davidi* sp. nov., male and female variability in PLE and PME width in relation to the ALE width shown in %; n = 25 females, 12 males.

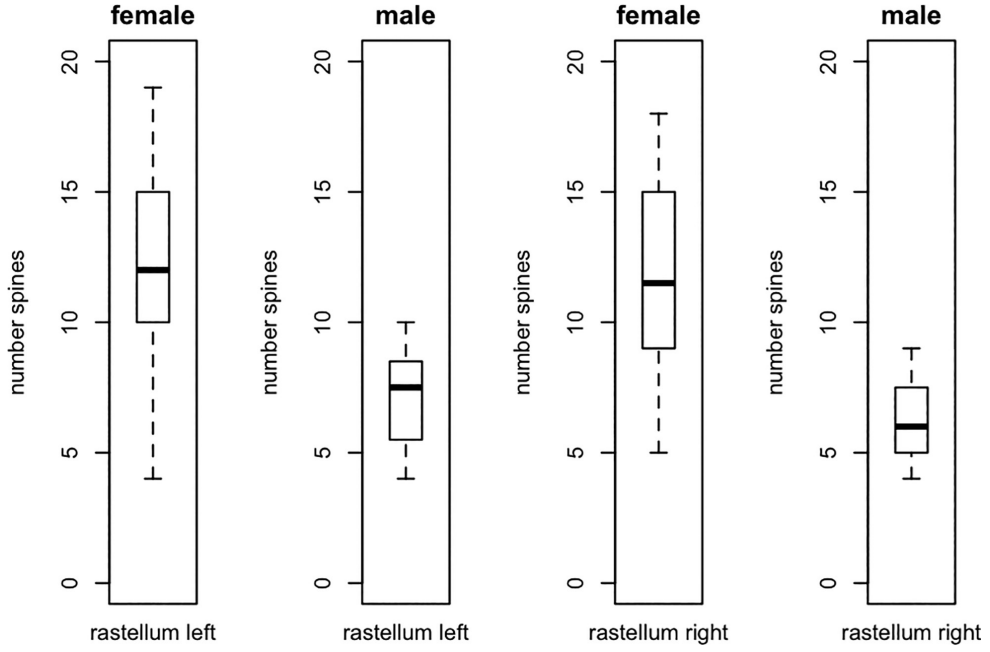

Figure 17. *Missulena davidi* sp. nov., male and female variability in number of spines on the rastellum; n = 26 females, 12 males.

available (e.g., *M. occataria*: no spines on patellae; see Wormesley, 1943). We emphasize that no single character is diagnostic alone and it is worth bearing this in mind when identifying or describing new species.

Although our phylogenetic analysis is based on a COI dataset rather than a multi-gene dataset that incudes additional nuclear markers, there may be several general implications. First of all, it is clear that *Missulena* is highly diverse at the genetic level (Fig. 2) with many more putative species awaiting detailed taxonomic assessment. This is not necessarily a new outcome since previous barcoding studies (e.g., Castalanelli et al. 2014; Harms and Framenau 2013; Framenau and Harms 2017) have highlighted high genetic diversity in the Western Australian fauna, and most *Missulena* species (including seven previously recovered synonyms; see Wormersley 1943; Main 1985) have been described from this state to date. However, the present tree adds many additional sequences and showcases striking patterns of diversity, particularly in the arid and semi-arid regions of Western Australia.

Secondly, it is evident that females are substantially more variable than males and species identification based on morphology is harder, if not impossible. This may be trivial but considering that we provide the first detailed description of female *Missulena* based on a large sample size, this reinforces what is already known in other lineages of trapdoor spiders in Australia (e.g., Atracidae: *Hadronyche*, Gray 2019; Halonoproctidae: *Conothele*, Huey et al. 2019; Idiopidae: various genera; e.g., Rix et al. 2018, 2019). Examining large series of specimens will help to better understand patterns of variability in all these taxa.

The third outcome is that variability in the characters examined is not simply an expression of isolation by distance at the genetic level but rather an expression of natural variability. Mitochondrial data alone have several limitations and the phylogenetic results given here may be affected by incomplete lineage sorting and/or even saturation at the deeper nodes of the phylogeny. However, we are assessing variability at shallow notes, in particular population structure, where the COI gene is clearly one of the most effective markers. Here it is interesting that there is substantial variation even within localised populations for several morphological characters we scored although COI sequences were (almost) identical. The examination of large specimen series will provide an account to such natural variability that may or may not have a genetic base in the nuclear genome.

Another outcome is that not necessarily all *Missulena* species have restricted ranges and that at least some species are quite widespread. This is perhaps not a surprising outcome given that several species, such as and *M. bradleyi* Rainbow, 1904, *M. occatoria* Walckenaer, 1905 and *M. dipsaca* Faulder, 1995, were always considered widespread (e.g., Wormersley 1943; Faulder 1995), but this assessment was based on morphology only and before molecular techniques revealed a highly diverse and often cryptic fauna of trapdoor spiders in Australia (e.g., Castallanelli et al. 2014).

One may argue in the case of *M. davidi* sp. nov. that both the genetic and morphological variability may point to a radiation of closely related species that are cryptic, similar to *Bertmainius tingle* (Main 1991) in southwestern Australia for which a dataset comprising two genetic markers (COI and ITS-2; see Cooper et al. 2011; Harvey et al. 2015) is available. The latter was once considered to be a single species with pronounced genetic divergences between localised populations but has since then be reclassified into seven species, each of which with very narrow distribution ranges and nuclear plus mitochondrial genetic differentiation (Harvey et al. 2015). In contrast to *Bertmainius*, morphological and genetic divergences in *M. davidi* sp. nov. do not correlate with spatial isolation of populations and morphological variability is distributed rather randomly across the four clades that we identified at the mtDNA level. *Missulena davidi* sp. nov. may be an interesting case of incipient speciation but morphology cannot be used to diagnose any of the four genetic clades against the other. These clades have overlapping distributions with a potential for geneflow. Bearing in mind the absence of spatial isolation between these clades, overlapping morphological character sets between these, and the lack of data about biology, behaviour, and ecological niche, we presently favour the hypothesis of a single species for *M. davidi* sp. nov.. This is despite the high genetic divergences of up to 22% that exceed previously considered barcoding thresholds to delineate mygalomorph spider species (e.g., 9.5% in Castalanelli et al. 2014; ~15% within *Aname mellosa*, Harvey et al. 2012) or values used in araneomorph spider species (partly reviewed in Abel et al. 2020). The high genetic divergences are shared with some other highly-structured arachnid species such as the harvestmen *Aokari denticulata* (19%; see Boyer et al. 2007) or schizomids (see Abrams et al. 2019, 2020). Our decision of a single species is made following the cohesion species concept as defined by Bond and Stockman (2008) who suggested a combination of character sets rather than single lines of evidence (genetics or morphology). *Missulena davidi* sp. nov. apparently represents an ongoing radiation in a dynamic landscape that has yet to evolve into morphologically (and perhaps biologically) discrete units.

Research using genomic tools could help further resolve the species boundaries in this radiation, providing a more robust molecular framework to test species concepts (e.g., Ivanov et al. 2021; Newton et al. 2020).

5. Acknowledgements

MG thanks Bennelongia Environmental Consultants (Jolimont, WA) and Stuart Halse in particular for supporting this research through a travel grant, the Western Australian Museum team for great company during her stay in 2019, Nadine Dupérré (LIB Hamburg) for technical support, and Tabea Schneider for company during the trip to Australia. All authors declare no conflict of interest. DNA sequencing of new specimens for this study was funded by the Gorgon Barrow Island Net Conservation Benefits Fund. The Fund is administered by the Department of Biodiversity, Conservation and Attractions and approved by

the Minister for Environment after considering advice from the Gorgon Barrow Island Net Conservation Benefits Advisory Board. We finally thank Robert Raven and Michael Rix (Queensland Museum, Brisbane) for reviewing earlier drafts of this manuscript.

6. References

Abel C, Schneider JM, Kuntner, M, Harms D (2020) Phylogeography of the 'cosmopolitan' orb-weaver *Argiope trifasciata* (Araneae: Araneidae). Biological Journal of the Linnean Society 131: 61–75. https://doi.org/10.1093/biolinnean/blaa078

Abrams KM, Huey JA, Hillyer MJ, Didham RK, Harvey MS (2020) A systematic revision of *Draculoides* (Schizomida: Hubbardiidae) of the Pilbara, Western Australia, Part I: the Western Pilbara. Zootaxa 4864(1): zootaxa.4864.1.1. https://doi.org/10.11646/zootaxa.4864.1.1

Abrams KM, Huey JA, Hillyer MJ, Humphreys WF, Didham RK, Harvey MS (2019) Too hot to handle: Cenozoic aridification drives multiple independent incursions of Schizomida (Hubbardiidae) into hypogean environments. Molecular Phylogenetics and Evolution 139: 106532. https://doi.org/10.1016/j.ympev.2019.106532

Bond JE, Stockman AK (2008) An integrative model for delimiting cohesion species: Finding the population-species interface in a group of Californian trapdoor spiders with extreme genetic divergence and geographic structuring. Systematic Biology 57: 628–646. https://doi.org/10.1080/10635150802302443

Boyer SL, Baker JM, Giribet G (2007) Deep genetic divergences in *Aoraki denticulata* (Arachnida, Opiliones, Cyphophthalmi): a widespread 'mite harvestman' defies DNA taxonomy. Molecular Ecology 16: 4999–5016. https://doi.org/10.1111/j.1365-294X.2007.03555.x

Buzatto BA, Haeusler L, Tamang N (2021). Trapped indoors? Long-distance dispersal in mygalomorph spiders and its effect on species ranges. Journal of Comparative Physiology A 207: 279–292. https://doi.org/10.1007/s0035 9-020-01459-x

Castalanelli MA, Teale R, Rix MG, Kennington WJ, Harvey MS (2014) Barcoding of mygalomorph spiders (Araneae: Mygalomorphae) in the Pilbara bioregion of Western Australia reveals a highly diverse biota. Invertebrate Systematics 28: 375–385. https://doi.org/10.1071/IS13058

Cooper SJ, Harvey MS, Saint KM, Main BY (2011) Deep phylogeographic structuring of populations of the trapdoor spider *Moggridgea tingle* (Migidae) from southwestern Australia: evidence for long-term refugia within refugia. Molecular Ecology 15: 3219–3236. https://doi.org/10.1111/j.1365-294X.2011.05160.x

Faulder RJ (1995) Two new species of the Australian spider genus *Missulena* Walckenaer (Araneae: Actinopodidae). Records of the Western Australian Museum, Supplement 52: 73–78.

Framenau VW, Baehr BC, Zborowski P (2014) A guide to the spiders of Australia. New Holland Publishers, London, Sydney, Auckland, 448 pp.

Framenau VW, Harms D (2017) A new species of Mouse Spider (Actinopodidae, *Missulena*) from the Goldfields region of Western Australia. Evolutionary Systematics 1: 39–46. https://doi.org/10.3897/evolsyst.1.14665

Gray MR (2010) A revision of the Australian funnel-web spiders (Hexathelidae: Atracidae). Records of the Australian Museum 62: 285–392.

Gunning SJ, Chong Y, Khalife AA, Hains PG, Broady KW, Nicholson GM (2003) Isolation of δ-missulenatoxin-Mb1a, the major vertebrate-active spider δ-toxin from the venom of *Missulena bradleyi* (Actinopodidae). FEBS Letters 554: 211–218. https://doi.org/10.1016/s0014-5793(03)01175-x

Harms D, Framenau VW (2013) New species of mouse spiders (Araneae: Mygalomorphae: Actinopodidae: *Missulena*) from the Pilbara Region, Western Australia. Zootaxa 3637: 521–540. https://doi.org/10.11646/zootaxa.3637.5.2

Harvey FSB, Framenau VW, Wojcieszek JM, Rix MG, Harvey MS (2012) Molecular and morphological characterisation of new species in the trapdoor spider genus *Aname* (Araneae: Mygalomorphae: Nemesiidae) from the Pilbara bioregion of Western Australia. Zootaxa 3383: 15–38. https://doi.org/10.11646/zootaxa.3383.1.3

Harvey MS (2002) Short-range endemism among the Australian fauna: some examples from non-marine environments. Invertebrate Systematics 16: 555–570. https://doi.org/10.1071/IS02009

Harvey MS, Main BY, Rix MG, Cooper, SJB (2015) Refugia within refugia: *in situ* speciation and conservation of threatened *Bertmainius* (Araneae: Migidae), a new genus of relictual trapdoor spiders endemic to the mesic zone of south-western Australia. Invertebrate Systematics 29: 511–553. https://doi.org/10.1071/IS15024

Harvey MS, Hillyer MJ, Main BY, Moulds TA, Raven RJ, Rix MG, Vink CJ, Huey JA (2018) Phylogenetic relationships of the Australasian open-holed trapdoor spiders (Araneae: Mygalomorphae: Nemesiidae: Anaminae): multi-locus molecular analyses resolve the generic classification of a highly diverse fauna. Zoological Journal of the Linnean Society 184: 407–452. https://doi.org/10.1093/zoolinnean/zlx111

Hedin M, Derkarabetian S, Ramírez MJ, Vink C, Bond JE (2018) Phylogenomic reclassification of the world's most venomous spiders (Mygalomorphae, Atracinae), with implications for venom evolution. Scientific Reports 8: 1636. https://doi.org/10.1038/s41598-018-19946-2

Huey JA, Hillyer MJ, Harvey MS (2019) Phylogenetic relationships and biogeographic history of the Australian trapdoor spider genus *Conothele* (Araneae: Mygalomorphae: Halonoproctidae): diversification into arid habitats in an otherwise tropical radiation. Invertebrate Systematics 33: 628–643. https://doi.org/10.1071/IS18078

Isbister GK (2004) Mouse spider bites (*Missulena* spp.) and their medical importance. A systematic review. Medical Journal of Australia 180: 225–227. https://doi.org/10.5694/j.1326-5377.2004.tb05890.x

Ivanov V, Marusik Y, Pétillon J, Mutanen M (2021) Relevance of ddRADseq method for species and population delimitation of closely related and widely distributed wolf spiders (Araneae, Lycosidae). Scientific Reports 11(1): 1–14. https://doi.org/10.1038/s41598-021-81788-2

Katoh K, Standley DM (2013) MAFFT multiple sequence alignment software version 7: improvements in performance and usability. Molecular Biology and Evolution 30: 772–780. https://doi.org/10.1093/molbev/mst010

Main BY (1956) Observations on the burrow and natural history of the trapdoor spider *Missulena* (Ctenizidae). Western Australian Naturalist 5: 73–80.

Main BY (1976) Spiders. Collins, Sydney, London. 296 pp.

Main BY (1985) Mygalomorphae. In Walton DW (ed.) Zoological Catalogue of Australia 3. Arachnida, Mygalomorphae, Araneomorphae in part, Pseudoscorpionida, Amblypygi and Palpigradi. Australian Government Publishing Service, Canberra, pp.1–48.

Miglio LT, Harms D, Framenau VW, Harvey MS (2014) Four new mouse spider species (Araneae, Mygalomorphae, Actinopodidae, *Missulena*) from Western Australia. ZooKeys 410: 121–148. https://doi.org/10.3897/zookeys.410.7156

Newton LG, Starrett J, Hendrixson BE, Derkarabetian S, Bond JE (2020) Integrative species delimitation reveals cryptic diversity in the southern Appalachian *Antrodiaetus unicolor* (Araneae: Antrodiaetidae) species complex. Molecular Ecology 29(12): 2269–2287. https://doi.org/10.1111/mec.15483

Nicholson GM, Walsh R, Little MJ, Tyler MI (1998) Characterisation of the effects of robustoxin, the lethal neurotoxin from the Sydney funnel-web spider *Atrax robustus*, on sodium channel activation and inactivation. Pflügers Archiv 436: 117–126. https://link.springer.com/10.1007/s004240050612

Oxford GS, Gillespie RG (1991) Evolution and ecology of spider coloration. Annual Review of Entomology 43: 619–643. https://doi.org/10.1146/annurev.ento.43.1.619

Palagi A, Koh JMS, Leblanc M, Wilson D, Sutertre S, King GF, Nicholson GM, Escoubas P (2013) Unravelling the complex venom landscapes of lethal Australian funnel-web spiders (Hexathelidae: Atracinae) using LC-MALDI-TOF mass spectrometry. Journal of Proteomics 80: 292–310. https://doi.org/10.1007/s004240050612

Rash LD, Birinyi-Strachan L, Nicholson GM, Hodgson WC (2000) Neurotoxic activity of venom from the Australian Eastern mouse spider (*Missulena bradleyi*) involves modulation of sodium channel gating. British Journal of Pharmacology 130: 1817–1824. https://doi.org/10.1038/sj.bjp.0703494

Raven RJ (1985) The spider infraorder Mygalomorphae (Araneae): cladistics and systematics. Bulletin of the American Museum of Natural History 182: 1–180.

Raven RJ (1994) Mygalomorph spiders of the Barychelidae in Australia and the western Pacific. Memoirs of the Queensland Museum 35: 291–706.

Rix MG, Raven RJ, Harvey MS (2018) Systematics of the giant spiny trapdoor spiders of the genus *Gaius* Rainbow (Mygalomorphae: Idiopidae: Aganippini): documenting an iconic lineage of the Western Australian inland arid zone. Journal of Arachnology 46: 438–472. https://doi.org/10.1636/JoA-S-17-079.1

Rix MG, Wilson JD, Harvey MS (2019) A revision of the white-headed spiny trapdoor spiders of the genus *Euoplos* (Mygalomorphae: Idiopidae: Arbanitinae): a remarkable lineage of rare mygalomorph spiders from the south-western Australian biodiversity hotspot. Journal of Arachnology 47: 63–76. https://doi.org/10.1636/0161-8202-47.1.63

Simon E (1903) Histoire naturelle des araignées. Deuxième édition, tome second. Roret, Paris, pp. 669–1080.

Stockman AK, Bond JE (2007) Delimiting cohesion species: extreme population structuring and the role of ecological interchangeability. Molecular Ecology 16: 3374–3392. https://doi.org/10.1111/j.1365-294X.2007.03389.x

Stamatakis A (2006) RAxML–VI–HPC: maximum likelihood-based phylogenetic analyses with thousands of taxa and mixed models. Bioinformatics 22: 2688–2690. https://doi.org/10.1093/bioinformatics/btl446

Starret J, Hedin M (2007) Multilocus geneaologies reveal multiple cryptic species and biogeographical complexity in the California turret spider *Antrodiateus riversi* (Mygalomorphae: Antrodiaetidae). Molecular Ecology 16: 583–604. https://doi.org/10.1111/j.1365-294X.2006.03164.x

Wong MKL, Woodman JD, Rowell DM (2017) Short-range phenotypic divergence among genetically distinct parapatric populations of an Australian funnel-web spider. Ecology and Evolution 7: 5094–5102. https://doi.org/10.1002/ece3.3084

World Spider Catalog (2020) World Spider Catalog. Version 21.5. Natural History Museum Bern, online at http://wsc.nmbe.ch, accessed on 1 April 2020. https://doi.org/10.24436/2

Womersley H (1943) A revision of the spiders of the genus *Missulena* Walckenaer 1805. Records of the South Australian Museum 7: 249–269.

Supplementary material 1

GenBank registration numbers

Authors: Greenberg MR, Huey JA, Framenau VW, Harms D (2021)
Data type: .xlsx
Explanation note: GenBank registration numbers and museum voucher numbers for all specimens that were sequenced in this study.

Link: https://doi.org/10.3897/asp.79.e62332.suppl1